Aerospace Science and Technology 121 (2022) 107395

Contents lists available at ScienceDirect

Aerospace Science and Technology

www.elsevier.com/locate/aescte

Conceptual design and comparative study of strut-braced wing and twin-fuselage aircraft configurations with ultra-high aspect ratio wings ☆

Yiyuan Ma *, Stanislav Karpuk, Ali Elham

Technische Universität Braunschweig, Braunschweig, 38108, Germany

ARTICLE INFO

Article history:
Received 3 October 2021
Received in revised form 28 December 2021
Accepted 27 January 2022
Available online 31 January 2022
Communicated by Mehdi Ghoreyshi

Keywords:
Ultra-high aspect ratio wing
Strut-braced wing
Twin-fuselage
Advanced airframe technology
Conceptual design

ABSTRACT

Sustainable and fuel-efficient next-generation air transportation demands a step change in aircraft performance. The ultra-high aspect ratio wings (UHARW) configuration is one key enabling strategy for improving aircraft aerodynamic efficiency and reducing fuel consumption and emissions. Unconventional aircraft configurations and advanced airframe technologies are required to address the large bending moment and shear stresses in the UHARW structure. This paper considers two promising unconventional configurations for adopting UHARW design, including strut-braced-wing (SBW) and twin-fuselage (TF), with advanced airframe technologies, i.e., active flow control, active load alleviation, and advanced airframe structures and materials. Three typical missions, including short-range (SR), medium-range (MR), and long-range (LR), are considered for aircraft design. A conceptual design and performance analysis framework for SBW and TF configurations is developed in this paper. According to the mission profile and top-level requirements proposed for each mission, an SBW and a TF configuration are designed, respectively. A comparative study is carried out to determine the best-in-class configuration of the corresponding mission to evaluate the potential of SBW and TF configurations for next-generation sustainable aviation applications. The results showed that the TF configuration has a better wing weight reduction effect than the SBW configuration, and the MR-TF and LR-TF aircraft have lower takeoff weight and fuel weight than those of the SBW aircraft for the same mission. However, due to the adjustment of the cabin dimensions for the SR-TF aircraft, the SBW configuration outperforms the TF configuration in this mission.

1. Introduction

Stringent sustainability goals for the next generation of commercial transport aircraft have been put forward by NASA [1] and European Commission [2] in recent years, including significant CO2, NOx, and noise reductions. In particular, in recovering the aerospace industry, which has been hit seriously by the unexpected COVID-19 pandemic, regaining its competitiveness, and addressing future climate goals, an unprecedented revolution in air transportation is required. Therefore, a step-change in aircraft performance is needed, for which the advancement in ultra-high aspect ratio wings (UHARW) configuration becomes one of the keys. In recent years, some efforts have been put forward to explore the benefits and potentials of UHARW, such as wingtip coupling, strut-braced wing (SBW), multi-fuselage, folding wings, etc. [3–5].

The wing bending moment of the UHARW is drastically larger than that of the conventional wings. Therefore, the wing structural weight penalty will be huge if there are no additional designs or structures to assist the UHARW. The strut of the SBW aircraft could reduce the maximum bending moment in the wing structure by significant amounts, typically up to 50%, which will significantly reduce the wing weight, thereby increasing the wingspan and reducing the wing thickness and sweep [6]. For this reason, many recent studies on UHARW have focused on the SBW configuration [6,7]. For example, the Subsonic Ultra Green Aircraft Research (SUGAR) team, consisted of NASA, Boeing, and the Georgia Institute of Technology, has comprehensively studied the SBW technology for the next-generation mid-range (MR) commercial transport aircraft [8].

Another promising concept for the UHARW is the twin/multi-fuselage configuration [5]. This aircraft configuration targets reduc-

☆ This paper has been modified from Y. Ma, S. Karpuk, and A. Elham, Conceptual design and comparative study of strut-braced wing and twin-fuselage aircraft configurations with ultra-high aspect ratio wings, AIAA AVIATION 2021 FORUM, 2-6 August 2021, VIRTUAL EVENT, AIAA Paper No. 2021-2425.

* Corresponding author.
E-mail addresses: yiyuan.ma@tu-braunschweig.de (Y. Ma), s.karpuk@tu-braunschweig.de (S. Karpuk), a.elham@tu-braunschweig.de (A. Elham).

https://doi.org/10.1016/j.ast.2022.107395

ing aircraft weight by two effects. The fuselages with their payloads are located away from the aircraft centerline, reducing the wing bending moment significantly. Moreover, twin-fuselage (TF) aircraft use the fuselage volume better than the single wide-body configuration for integrating passengers on large aircraft, thereby reducing fuselage weight by up to 40% [9]. The TF concept has already been realized in large aircraft and unmanned aerial vehicles (UAVs), such as a TF UAV [10], a general aircraft HY4 [11], WhiteKnightTwo [12], etc. However, this concept still has not been investigated in detail for transport passenger aircraft, probably due to airport infrastructure constraints (e.g., runway width and terminal access).

There have been numerous projects and research on UHARW aircraft, including the SBW configuration, the TF configuration, etc. However, current research on UHARW aircraft configurations and missions is not comprehensive enough. For example, the SUGAR project did a comprehensive study on the MR-SBW passenger aircraft, but it focused only on the SBW concept and did not consider short-range (SR) and long-range (LR) missions. Virginia Polytechnic and State University [13] conducted the conceptual design and optimization research for a long-range SBW passenger aircraft in the same manner. Besides, there is few comprehensive research on TF passenger aircraft that has been published. Therefore, a conceptual design and comparative study of SBW and TF configurations for typical SR, MR, and LR missions are necessary to comprehensively explore the possibility of adopting SBW and TF configurations in next-generation air transportation.

Numerous studies on advanced airframe technologies are being conducted for the next-generation transport aircraft in aerodynamics, structure, materials, etc., which are expected to reach a high technology readiness level (TRL) and be widely used in the next-generation transport aircraft in the not-too-distant future [14]. The advanced airframe technologies considered in this work include hybrid laminar flow control (HLFC), load alleviation, and advanced materials and structure.

Natural laminar flow (NLF) can reduce viscous wing drag for SR and MR aircraft significantly [15]. However, maintaining a large NLF range on the large aircraft wings is difficult due to their high wing sweep angles. For this reason, HLFC can be integrated into wings and tails to delay flow transition [16], i.e., the laminar boundary of wings and tails is also extended by the boundary layer flow control technology, which allows a much higher percentage of the laminar flow range and has the potential to reduce the overall aircraft drag by up to 50% [15]. Aircraft structures need to be sized according to the maximum load factors. Aircraft design calculations indicate that the wing weight savings are in the order of 45% if the maximum load factors can be reduced to +1.5 g and -0.5 g by advanced load alleviation systems [17]. Load alleviation introduces various techniques to reduce the loads experienced by aircraft and allows for a lighter wing design, which consists of passive load alleviation and active load alleviation techniques [14,17]. Over the past decades, composites have gradually replaced traditional metallic material in aircraft structures. For the next-generation transport aircraft, tow steering [18] and thin ply materials [19] are promising technologies that are expected to reduce composite fiber reinforced polymers (CFRP) structures' weight by 15% and 10%, respectively, compared to conventional composite structures. These advanced technologies need to be considered and assumed at the aircraft initial sizing stage to study the potential impact of introducing these technologies on the flight performance of the researched unconventional aircraft configurations.

Robust- and sustainable-by-design ultra-higH aspEct ratio wing and Airframe (RHEA) is a European Union-funded project within the Clean Sky 2 Joint Undertaking (rhea-cleansky2.org/). The RHEA team consists of Technische Universität Braunschweig (DE), University of Strathclyde (UK), Imperial College (UK), DNW Wind Tunnels (NL), and IRT-Saint Exupery (FR), aiming at conceiving innovative next-generation aircraft configurations capable of accelerating the readiness of UHARW by integrating advanced technologies under the paradigm of robustness- and sustainability-by-design [20]. The RHEA project's top-level goals are listed in Table 1. A rendering of the mid-range SBW configuration and TF configuration with UHARW designed by the authors in the RHEA project is shown in Fig. 1.

Table 1
RHEA project goals.

Aerodynamics (L/D)	+50 %
Research and development costs	-5 to -10 %
Fuel weight / Emissions (CO2, NOx)	-40 %
Noise	-2 to -4 dB

Fig. 1. SBW and TF configurations of RHEA mid-range mission.

This paper presents the conceptual design and comparative study of the SBW and TF aircraft configurations with UHARW design for three different classes of aircraft, including short-range, mid-range, and long-range. A conceptual design and analysis framework for the SBW configuration and TF configuration with advanced airframe technologies is developed by integrating and improving several methods and tools. Corresponding to the proposed mission profile and top-level requirements, an SBW configuration and a TF configuration are designed for each mission, and a comparative study is conducted between the two configurations. Finally, the best-in-class aircraft configuration for each of the three proposed missions is determined so that the potential of SBW and TF configurations for next-generation air transportation applications is evaluated through comparative studies at the conceptual design phase.

2. Methodology for conceptual design and analysis

2.1. Conceptual design environment

PyInit [14], an in-house aircraft initial sizing tool developed by the authors, is used for the initial sizing and performance evaluation of the RHEA aircraft. PyInit contains numerous semi-empirical formulas and physics-based analysis methods for the constraint diagram sizing, components sizing, aerodynamic analysis, static stability, control analysis, propulsion sizing, flight performance evaluation, etc. Several modules and functions in PyInit, such as frictional drag estimation and component sizing, are modified in this paper, accounting for the SBW and TF aircraft configurations. Initial sizing in PyInit starts from analyzing constraints according to the top-level requirements. Then wing loading and thrust-to-weight ratio can be determined corresponding to the constraint diagrams, and the components, including the wing, fuselage, and tails of the aircraft, can be sized. Finally, various analyses, such as aerodynamics, stability, control, and performance characteristics, can be performed.

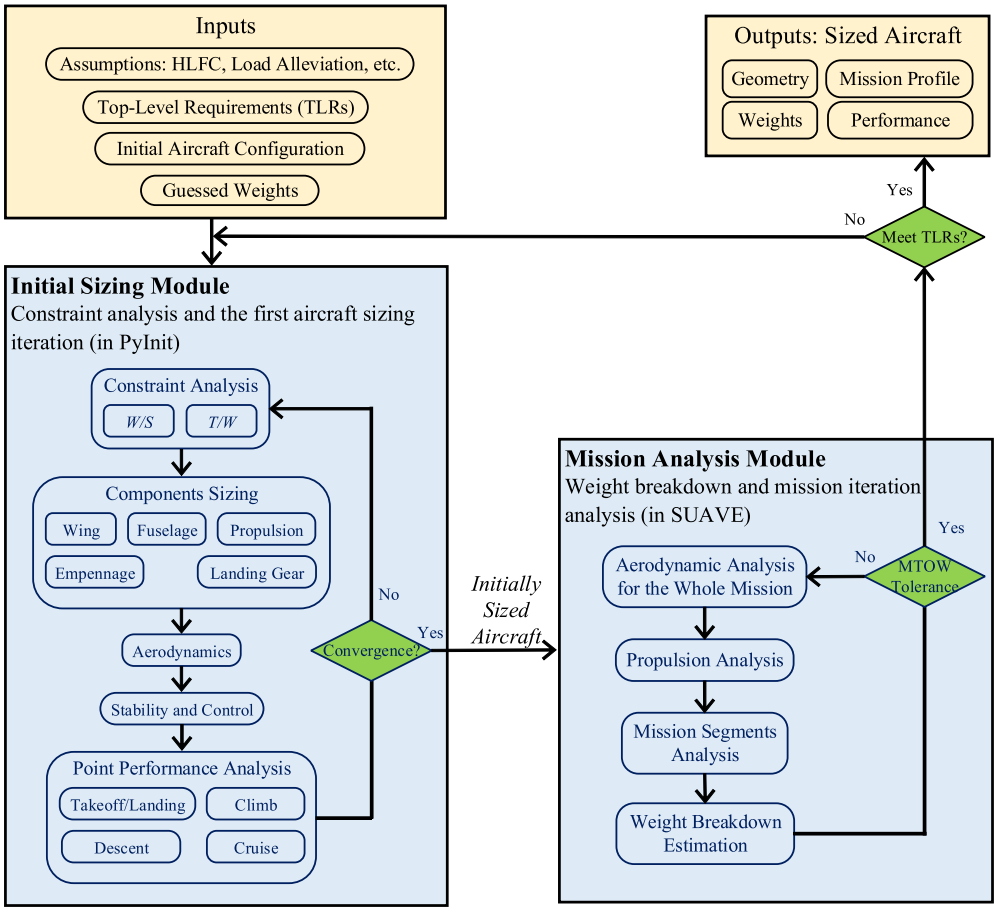

Fig. 2. RHEA aircraft sizing and analysis procedure.

Then, the initially sized aircraft is imported into the open-source aircraft assessment tool Stanford University Aerospace Vehicle Environment (SUAVE) [21] for the multi-fidelity analysis on the weight breakdown, aerodynamics, flight performance, and missions through convergent iterations. SUAVE contains the analysis modules for several unconventional aircraft configurations, such as solar-powered UAVs, electric vertical takeoff and landing (eVTOL) aircraft, etc. However, so far, SUAVE does not include analysis modules for SBW and TF concepts. Therefore, SUAVE is modified and improved in this research by adding modules on the impact of introducing the above-mentioned advanced technologies and analyzing SBW and TF aircraft configurations, including weight breakdown and parasitic drag estimation methods. In particular, the wing weight estimation methods for SBW and TF aircraft configurations are the most concerned. A class II wing weight estimation method for SBW aircraft developed by Chiozzotto [22], which considers CFPR materials and aeroelastic effects, is used in this paper for the SBW aircraft sizing. A physics-based wing weight estimation method for TF aircraft developed by Udin [23] is improved and used for TF aircraft sizing. These two unconventional wing weight estimation methods are integrated into the weight analysis module of SUAVE for RHEA aircraft performance analysis.

UHARW aircraft has a problem regarding compliance with the airport dimensional restrictions. For example, corresponding to the International Civil Aviation Organization (ICAO) Class C restriction, the wingspan of the mid-range passenger aircraft cannot exceed 36 meters, and the main landing gear span cannot exceed 9 meters. Therefore, making the wing foldable is essential, and the wing weight penalty due to the wing folding should be taken into account. The estimation method of wing mass penalty due to the folding-wing mechanisms represented in Ref. [24] is used in this work.

OpenVSP [25] and CATIA are used for aircraft geometric modeling and visualization.

The sizing and analysis process for RHEA aircraft established in this research is shown in Fig. 2. The procedure starts with the initial sizing module using PyInit, which performs constraint analysis using several semi-empirical formulas and physics-based analysis methods to determine the aircraft's wing loading, thrust-to-weight ratio, and component geometry by estimating aerodynamic performance for high/low-speed configurations, point performance analysis, etc. As introduced, PyInit is an initial sizing tool for obtaining initial aircraft configurations and geometric components, such as wing platform and tail volume ratios, but not aircraft weight and mission segments convergent iterations. Therefore, after this, the initially sized aircraft is transferred to the mission analysis module for iterative calculations, where the aircraft geometry and weights are modified by SUAVE to meet the mission segment requirements, i.e., the analysis in SUAVE, such as aerodynamic estimation, is performed for the aircraft's different configurations according to each mission segment (e.g., climb, cruise, descent, etc.) and for the updated aircraft geometry after each iteration.

2.2. Initial sizing method for SBW aircraft

2.2.1. Weight estimation

In general, aircraft maximum take-off weight (MTOW) can be written as

$$m_{TO} = m_{crew} + m_{pay} + m_f + m_e \tag{1}$$

where m_{TO} is the MTOW, m_{crew} is the crew mass, m_{pay} is the payload mass, m_f is the fuel mass, and m_e is the empty mass.

In Eq. (1), m_{crew} and m_{pay} are obtained from the top-level aircraft requirements (TLAR). m_f can be estimated by using the Breguet range equation or physics-based method with respect to the TLAR. The main difference between SBW aircraft weight estimation and that of conventional aircraft is m_e. For the structural weight estimation of SBW aircraft components except for wings, i.e., fuselage, tailplanes, engines, landing gears, etc., traditional weight estimation methods such as FLOPS [26] can be used. For estimating the wing weight, a semi-empirical method developed specifically for the conceptual design of SBW aircraft presented in Ref. [22] is used. This method was developed based on a physics-based wing weight estimation tool. Aileron efficiency and aeroelastic divergence effects on the wing weight are considered. The wing mass in this method is given by:

$$m_w = k_{ail}\left(m_{covers} + m_{webs+ribs}\right) + m_{sec} + m_{strut} \tag{2}$$

where m_w is the total mass of the wing and strut, m_{covers} is the wing box covers mass, including skins, stringers, and non-optimal mass penalties, $m_{webs+ribs}$ is the wing box spar webs and ribs mass, m_{sec} is the secondary wing structures mass, m_{strut} is the strut and juries mass, and k_{ail} is the wing box mass penalty factor due to aileron efficiency constraints. All masses in Eq. (2) are in kg. m_{covers}, $m_{webs+ribs}$, and m_{strut} can be calculated by

$$m_{covers} = k_e \cdot C \cdot m_{TO}^{E_e}(W/S)^{E_{ws}} AR^{E_A}(\cos\Lambda)^{E_\Lambda}(t/c)^{E_t} V^{E_V}(1+\lambda)^{E_\lambda} n_z^{E_{nz}}(1-\eta)^{E_\eta} \tag{3}$$

$$m_{webs+ribs} = k_e \cdot C \cdot m_{TO}^{E_e}(W/S)^{E_{ws}} AR^{E_A}(\cos\Lambda)^{E_\Lambda}(t/c)^{E_t} V^{E_V}(1+\lambda)^{E_\lambda} n_z^{E_{nz}}(1-\eta)^{E_\eta} \tag{4}$$

$$m_{strut} = k_e \cdot C \cdot m_{TO}^{E_e}(W/S)^{E_{ws}} AR^{E_A}(\cos\Lambda)^{E_\Lambda}(t/c)^{E_t} V^{E_V}(1+\lambda)^{E_\lambda} n_z^{E_{nz}}(1-\eta)^{E_\eta} P_{st}^{E_{pst}} \tag{5}$$

where k_e is the engine relief factor, W/S is the wing loading at takeoff, AR is the wing aspect ratio, Λ is the wing sweep angle ($c/2$), t/c is the airfoil thickness ratio, V is the maximum operating speed (equivalent speed, m/s), λ is the wing taper ratio, n_Z is the design maximum positive load factor, η is the normalized strut attachment position, P_{st} is the strut parameter, and different constant C and exponents E are used for each equation. The values of these parameters for different materials (aluminum and composites) and different configurations, including backward swept SBW and forward-swept SBW, are given and described in detail in Ref. [22].

2.2.2. Wing sizing

The main advantage of the SBW configuration is that it can be designed with a high (or even ultra-high) aspect ratio wing and therefore the induced drag can be reduced significantly. Besides, due to the strut's support, the thickness-to-chord ratio of wing airfoils can be reduced, and thus the compressive drag and pressure drag can be reduced.

As mentioned above, since there is a lot of research on natural laminar flow and hybrid laminar flow control techniques and some of them have yielded promising results, the influences of such techniques on the wing and airfoil design need to be considered. For example, the wing leading edge sweep angle should not exceed 18 degrees to limit4 the transversal instabilities of the airflow on the wing [27]. If the SBW aircraft will operate in the transonic region, supercritical airfoils shall be used. Otherwise, natural laminar airfoils can be selected. And according to the SBW characteristics, the maximum thickness-to-chord ratio can be initially chosen to be around 10-12% [8,27]. Moreover, in terms of aerodynamics, structures, mass properties, etc., the wing thickness can be held constant from the wing root to the strut attachment position, the maximum thickness-to-chord ratio can be held constant between the strut attachment position and the wing folding position (if applicable), and conventional wing thickness-to-chord ratio distributions can be applied to the outboard wing segment [8].

2.2.3. Strut sizing

In general, the strut is considered as a structural element without any lift contribution to the aircraft at cruise because any significant amount of lift produced on the strut would have an adverse impact on the wing structure. From a structural point of view, the strut can be designed in a spindle shape, since the chord is sized by buckling, which is not critical at the attachment position. The strut is designed to be attached to the wing front spar and the other end is attached to the main landing gear attachment structure of the fuselage. The strut uses a symmetric airfoil and the airfoil thickness-to-chord ratio can be calculated as the wing t/c plus $0.05/\cos(\Lambda)$, but not greater than 20% [22].

Recently, the SUGAR team studied the potential of considering the strut as a primary lifting surface rather than a purely structural element by staggering the wing and strut (root) thereby creating the potential for the strut to contribute more significantly to the aerodynamic performance of the aircraft [28]. The design space of different strut airfoils (NLF and conventional airfoils) combined with different strut loading was explored in Ref. [29] and results showed that an aircraft with a higher Mach number ($Ma = 0.80$ vs. $Ma = 0.73$) may benefit from loading the strut due to compressibility effects on the wing, i.e., lowering the sectional wing lift coefficient can help reduce shock formation and the compressive drag coursed by it. Otherwise, the strut is better to serve as a purely structural member to limit drag contribution. It should be noted that for the strut loading design, the load distribution on the strut needs to be carefully designed, i.e., the strut twist tailoring is very important.

Zhang et al. [30] developed a wing aero-structural analysis method for SBW aircraft and investigated the effect of strut attachment position on the structural weight, and results showed that the optimal strut attachment position is between 60% and 70% of the wingspan.

2.2.4. Validation

The SUGAR aircraft with a high aspect ratio wing was selected for the SBW aircraft analysis module validation. The SUGAR aircraft, featuring an SBW configuration, was designed for the mid-range mission with 154 passengers (2 class) and a range of 3500 nm, which has been studied in detail by high-fidelity aerodynamic and structural analysis and wind tunnel experiments [28]. The SUGAR aircraft data required for the analysis were extracted from Ref. [8]. The payload, range, and geometric parameters of SUGAR aircraft were input into the modified SUAVE, and the calculations were iterated until the weight and mission segments are converged. The comparison of the SUGAR aircraft and the resulted aircraft by SUAVE are tabulated in Table 2. It can be seen that the presented modified SUAVE has a good accuracy of weight estimation for this SBW aircraft, with relative errors below 2%, while the aerodynamic data show relatively high errors, mainly due to: 1) a drag bookkeeping method incorporating the wing-body computational fluid dynamics (CFD) solutions are used in the SUGAR aircraft aerodynamic analysis [8], while a relatively low fidelity method Fidelity Zero [21] is used in SUAVE tool for the concep-

Table 2
Validation of the SBW analysis module in the modified SUAVE.

Group	SUAVE result	SUGAR [8]	Relative error/%
MTOW, kg	66998	68039	-1.53
Fuel weight, kg	15599	15365	1.52
Empty weight, kg	36799	36328	1.30
C_L	0.685	0.750	-8.67
C_D	0.0290	0.0298	-2.58
C_{D_0}	0.0218	0.0200	8.99
C_{D_i}	0.0107	0.0098	8.77
L/D	23.5882	25.159	-6.24

The aerodynamic data listed here are for the midpoint of cruise corresponding to 50% fuel.

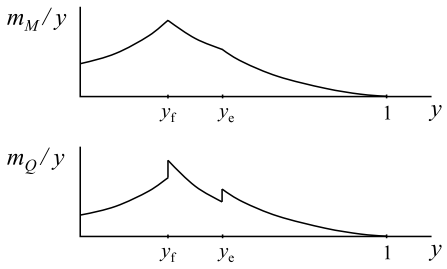

Fig. 3. Spanwise distribution of relative wing mass for TF aircraft [23].

tual design phase aerodynamic estimation; 2) the SUGAR aircraft uses supercritical airfoils specially designed by Boeing using its in-house tools [8], and the airfoils' geometric details are not publicly available. So the similar supercritical airfoils with the same thickness-to-chord ratio as the SUGAR aircraft are selected for the wing root, kink, and tip, and the same wing laminar flow area as SUGAR is assumed. Therefore, a relative difference of about 8% in some aerodynamic data is considered acceptable at the conceptual design stage.

2.3. Initial sizing method for TF aircraft

2.3.1. Weight estimation

The most significant difference between TF aircraft and conventional aircraft in sizing is the wing mass estimation, since the loads' spanwise distribution on the wing is significantly different, as shown in Fig. 3. While traditional semi-empirical weight estimation methods, such as FLOPS [26], can be used for other components' weight estimation, including fuselages, tailplanes, engines, etc.

Although the finite element method (FEM) is highly adaptable and accurate for wing mass estimation, especially for unconventional aircraft wings, it requires more information and is time-consuming, outweighing its benefits at the conceptual design stage. A semi-analytical wing mass estimation method for TF aircraft developed by Udin [23] is used in this study, and the wing structural mass is calculated through integrating the wing spanwise mass distribution, including wing structural mass, fuel mass, and concentrated mass, with the aerodynamic load. In this method, each fuselage is assumed as a concentrated load, including all weights not located on the wing. The relative wing structural mass can be expressed as

$$m_s = k_{sl} k_{tw} k_{man} \left(m_M + m_Q \right) + m_{rib} + m_{sec} \tag{6}$$

where the service life factor k_{sl}, the twist moment factor k_{tw}, and the manufacturing factor k_{man} can be determined by referring to Ref. [23]. m_{rib} is the relative mass of wing ribs, m_{sec} is the relative mass of wing secondary components, and m_M and m_Q are the estimated relative structural mass counteracting the wing bending moment and shear force, which can be given by

$$m_M = \frac{\rho n_z g}{\delta_u T_r} \frac{b^2}{2} E_T \int_0^1 \frac{Mo_{sum}}{P(y) \cos \Lambda} \, dy \tag{7}$$

$$m_Q = \frac{\rho n_z g}{\delta_{us}} \frac{b}{2} \int_0^1 \frac{Q_{sum}}{\cos \Lambda} \, dy \tag{8}$$

where Mo_{sum} and Q_{sum} are the total reduced wing bending moment and total reduced shear force caused by the loads on the wing. The detailed calculation and derivation process can be found in Ref. [23].

It should be noted that the presented TF aircraft wing mass estimation method was developed in the last century and only metallic materials were considered. Since this project targets the next-generation passenger aircraft, and CFRP materials will be the main material for the next-generation aircraft wings, this wing mass estimation method needs to be improved for CFRP materials. In the preliminary design, the cut-off strain method can be used for the composite wing structural sizing, which is determined corresponding to the worst of all situations [31]. This method combined with the 10% rule [32] is used to calculate the allowable for composite materials. The calculation method for the laminate properties of composite materials developed by the authors presented in Ref. [31] is used to estimate the maximum allowable stresses in the wing box upper and lower panels and the maximum buckling stresses and shear stresses in the front and rear spars.

2.3.2. Wing sizing

The wing of a TF aircraft is divided into two segments by the off-centerline located fuselages. Since the landing gears of TF aircraft can be stowed underneath the fuselage cabin floor and external fairings are not necessary for the main landing gears, the wing root section does not need to be modified in terms of the landing gear fairings.

In designing a wing, it is important to find the balance between aerodynamic and structural considerations, especially for the center wing segment of TF aircraft. From the structural point of view, a non-swept center wing segment is preferred, which also facilitates the achievement of laminar flow control. In contrast, a swept center wing segment will introduce the transversal instabilities of the airflow, which will aggravate the adverse aerodynamic interaction of the wing with two fuselages. Therefore, for TF aircraft operating at not very high Mach numbers, a non-swept center wing segment is recommended and advanced supercritical airfoils (if operating at transonic region) should be utilized to limit the compressive drag of the center wing segment. Subsequently, after the aerodynamic analysis, the compressive drag of the center wing segment should be evaluated to check if the amount is acceptable, and if not, the center wing segment needs to be modified to a swept design.

2.3.3. Fuselage sizing

The fuselage sizing process of TF aircraft consists of three steps: initial geometric sizing, cabin interior arrangement, and cargo capacity check [33].

In the initial sizing stage, the reference aircraft's fuselage can be used as the reference for the TF aircraft fuselage sizing. The same total floor area as the reference conventional aircraft can be taken as the sizing criterion for TF passenger aircraft to ensure the same number of passenger seats, while the same total fuselage volume can be used as the sizing criterion for TF cargo aircraft design. As shown in Fig. 4, in order to have the same floor area, the length and equivalent diameter of each fuselage of TF aircraft should be divided by $\sqrt{2}$, respectively.

Corresponding to the scaling method illustrated in Fig. 4, the fuselage fitness ratio does not change. The number of seats per

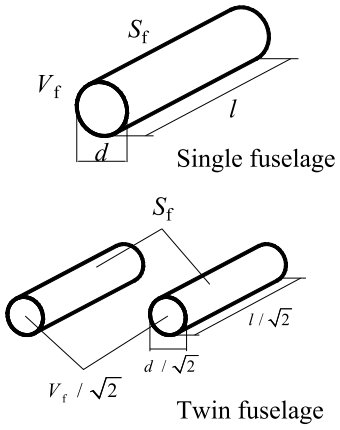

Fig. 4. The TF concept has the same floor area as the single-fuselage concept [9].

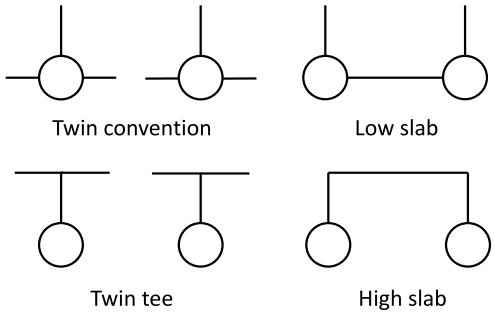

Fig. 5. Alternative tailplane configurations [33].

row of TF aircraft should also be initially determined by dividing the value of the reference fuselage by $\sqrt{2}$. And then the cabin parameters, including aisle height, aisle width, seat pitch, seat width between the armrests, etc., need to be checked in detail according to the Certification Specification 25 (CS 25) [34] and recommendations in Refs. [9,35]. If any of the parameters do not meet the requirements, the fuselage geometry will need to be adjusted within reasonable limits.

The next step is to check the cargo capacity. Since the same total floor area is used as the sizing criterion, the cargo capacity of TF aircraft is lower than that of the single-fuselage aircraft ($\sqrt{2}$ times smaller), as shown in Fig. 4. Therefore, it is necessary to check if the cargo hold capacity meets the design requirements. For example, the cargo capacity needs to be no less than 23 kg per passenger. Otherwise, the fuselage needs to be modified to increase the cargo hold capacity.

2.3.4. Tailplane configuration

There are several alternative tailplane configurations for TF aircraft [33], as shown in Fig. 5. And these four configurations can be divided into the high-horizontal tail layout and low-horizontal tail layout. Due to the short fuselage length of TF aircraft, larger horizontal and vertical tails are required. Therefore, the high-horizontal concept is more recommended since it increases the tail moment arm so as to reduce the tailplane's weight. Besides, the high-horizontal tail configuration allows the horizontal tail to avoid the downwash flow from the high wing.

Due to the endplate effect of vertical tails or fuselages and the higher aspect ratio allowed, the horizontal slab tails have better aerodynamic efficiency, resulting in a smaller horizontal tail area and lighter structure. However, this concept imposes additional asymmetric loads on vertical tails during maneuvering flight. Therefore, if a horizontal slab tail configuration is used, a high-fidelity finite element method is required to evaluate the weight penalty of vertical tails in the subsequent preliminary design stage.

Table 3
Validation of the TF analysis module in the modified SUAVE.

Parameter	SUAVE	Reference value [36]	Error, %
MTOW, kg	863885	891128	-3.06
OEW, kg	314174	335250	-6.29
Fuel Weight, kg	199732	205900	-2.99
C_L	0.485	0.509	-4.72
C_D	0.0226	0.0220	2.64
L/D	21.48	23.14	-7.17

The aerodynamic data listed here are for the midpoint of cruise corresponding to 50% fuel.

2.3.5. Validation

A large cargo TF aircraft designed by Lockheed and NASA to replace the Lockheed C-5A and the Boeing 747 transport aircraft was chosen to validate the TF aircraft analysis module in the modified SUAVE. The technology assumptions and required data were extracted from Ref. [36], and a comparison of the reference aircraft and the resulted aircraft are listed in Table 3, which shows an acceptable accuracy.

3. Conceptual design and comparative study

In this section, an SBW configuration and a TF configuration are designed for each mission, i.e., a total of 6 aircraft are designed in the following subsections. Comparative studies are carried out to determine the best-case and worst-case configurations for each mission.

3.1. Overview of design requirements and assumptions

RHEA aircraft is designed to comply with CS-25 certificate regulations [34]. ATR 72-600, A320neo, and B777-300ER are selected as the baseline reference aircraft for short-, mid-, and long-range missions, respectively. The EIS of RHEA aircraft is taken as the year 2040.

As introduced in Section 1, RHEA aircraft will be designed with a UHARW configuration. Referring to some future aircraft designs [8,18,37], the RHEA aircraft's wing aspect ratio is initially taken as 25 in the initial conceptual design stage, which will be optimized in the later optimization study phase.

As described in Section 1, several advanced airframe technologies of the next-generation passenger aircraft need to be considered in this research. The assumptions of the above-mentioned advanced airframe technologies for each mission and each configuration are tabulated in Table 4.

The mission profile of RHEA aircraft is shown in Fig. 6. The entire mission is divided into several segments, including the main mission and a reserve phase. For the reserve flight, the current requirements for mid-range passenger aircraft are 5% of trip fuel, a 200 nm divert segment, and a 30 min hold [38]. However, considering the aircraft studied in this research will operate in the future environment, these requirements are expected to be reduced based on the assumption that the air traffic control technology will be improved by then, and the assumed values for each mission will be shown in the following subsections.

3.2. Medium-range mission

As medium-range mission is currently the most concentrated research field for the next-generation passenger aircraft, this research starts with this mission because there are abundant reference aircraft.

Table 4
Assumptions of advanced airframe technologies used in the conceptual design.

Configuration		HLFC (Percentage of laminar flow area on the wing and tailplane)	Load alleviation (max. load factors)	Advanced materials & structures
Short-range	SBW	65%	+1.5 g and -0.5 g	20% structural weight reduction
	TF	70%		
Mid-range	SBW	50%	+1.5 g and -0.5 g	20% structural weight reduction
	TF	55%		
Long-range	SBW	50%	+1.5 g and -0.5 g	20% structural weight reduction
	TF	55%		

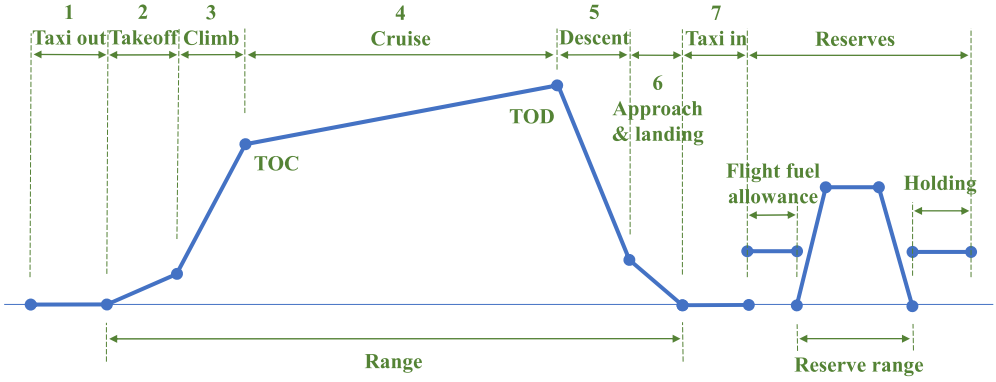

Fig. 6. RHEA aircraft mission profile.

Table 5
Top-level requirements of the mid-range mission.

Parameter		Unit	RHEA	References			
				SUGAR [8]	SE2A [14]	D8.5 [37]	SD8.5 [1]
Reference aircraft		–	A320neo	B737NG	A320	B737-800	B737-800
Cruise Mach number		–	0.78	0.71	0.78	0.74	0.74
Max. Mach number		–	0.82		0.82		
Passengers (1 class)		–	186		186	180	180
Passengers (2 class)		–	150	154	150		
Range		nm	3400	3500	2490	3000	3000
Reserves	Contingency fuel	–	3%	3%	5%	5%	5%
	Divert segment	nm	200	200	200		
	Hold (at 1500 ft)	min	10	10	30		
Cruise altitude		ft	33000	Vary	35000	44653 to 46415	44653 to 46415
Service ceiling		ft	38500	43000	37000		
Takeoff field length		ft	<6400	<8190	<6000	5000	4850
Landing distance		ft	<4500		<4500	3555	
Approach speed		kt	136	135	140		
Airport (ICAO C)	Wingspan	m	36	36	36		
	Main landing gear span	m	9				
Certification regulation		–	CS 25	FAR 25	CS 25	FAR 25	FAR 25

3.2.1. Initial aircraft sizing

Several high aspect ratio wing aircraft, including SUGAR aircraft [8], SE2A mid-range aircraft [14], D8.5 aircraft [37], and SD8.5 aircraft [1], were chosen as the reference for the RHEA mid-range aircraft design and comparison. A320neo aircraft was selected as the baseline aircraft for the RHEA mid-range mission, and the top-level requirements of RHEA mid-range aircraft were mainly referred to that of A320neo. The top-level requirements of the RHEA mid-range mission and that of the selected reference aircraft are listed in Table 5.

Reducing the cruise Mach number can bring benefits for aircraft fuel efficiency [8]. Therefore, several next-generation passenger aircraft research slightly decreased the design cruise Mach number, such as SUGAR and D8 aircraft, as given in Table 5. However, since the RHEA project focuses on the advantages/differences of introducing ultra-high aspect ratio wing and advanced airframe technologies for the next-generation passenger aircraft, the cruise and maximum Mach number are the same as those of the baseline aircraft A320neo, for comparison purposes. The fuel efficiency improvement effect of reducing cruise Mach number will be investigated at a later stage. As RHEA aircraft is designed with UHARW, it should be noted that there are regulations for the aircraft wingspan due to the airport facilities constraints [8]. For the mid-range aircraft operating at ICAO Class C airports, the wingspan constraint is 36 m, and the outer main gear wheel span should not exceed 9 m which is an important constraint for the TF configuration sizing.

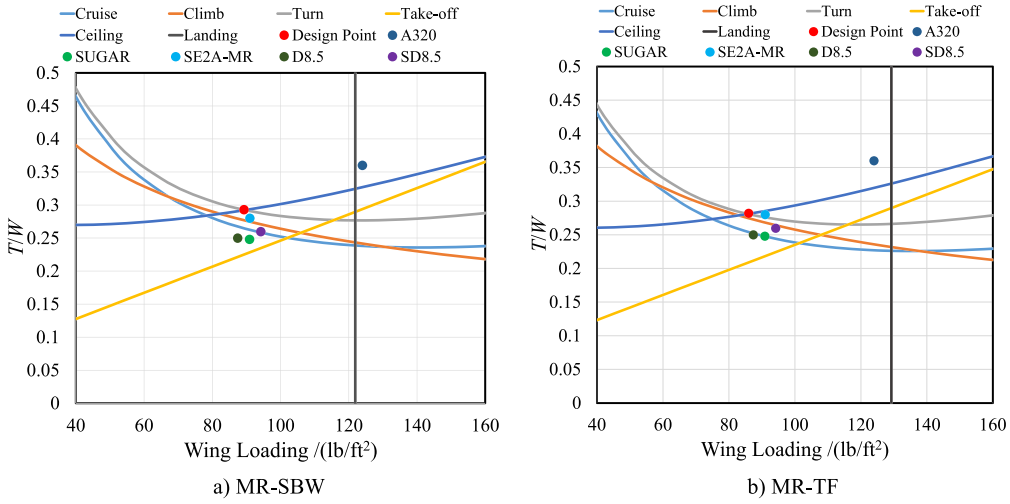

Fig. 7. RHEA-MR aircraft constraint diagrams. (For interpretation of the colors in the figure(s), the reader is referred to the web version of this article.)

The advanced airframe technology assumptions are given in Table 4, which were applied to PyInit and SUAVE during the MR aircraft conceptual design and performance assessment.

As described in Section 3, the aircraft initial sizing tool PyInit, modified for SBW and TF concepts in this research, was used for the initial sizing of the MR-SBW and MR-TF aircraft. Corresponding to the top-level design requirements and advanced technology assumptions given in Table 4 and Table 5, the wing loading and thrust-to-weight ratio of the MR-SBW and MR-TF aircraft were sized, and the design points are shown in Fig. 7. Besides, the design points of the selected reference aircraft are also shown in Fig. 7 for comparison.

OpenVSP was used for the visualization of the initially sized aircraft configurations. The three-view dimensions of the aircraft are shown in Fig. 8. Considering the UHARW concept, both the MR-SBW and MR-TF aircraft feature a high-wing configuration with two wing-mounted high bypass ratio turbofan engines. The wings are designed to be foldable with the folding position being 36/2 m of the half-wingspan. The supercritical airfoils NASA SC(2)-0412 and NASA SC(2)-0410 were adopted for the wing root and wingtip airfoil, respectively, and NASA SC(2)-0010 was used for the tailplane airfoil. Besides, the wing sweep angle (0.25c) was taken as 12.5 deg, which is a trade-off between laminar flow maintenance and compressive drag.

A T-tail was chosen for the MR-SBW aircraft due to the high-wing configuration. The strut was designed to be attached at 49.79% of the half-wingspan position. The chord of the strut is sized by buckling, resulting in the strut being shaped like a spindle [8].

The high-slab configuration was used for the MR-TF aircraft tailplanes. The horizontal tail was designed with a forward-swept configuration, which can increase the horizontal tail moment arm to reduce the horizontal tail area and reduce the wave drag of the horizontal tail (compared to a zero-swept horizontal tail).

To facilitate comparison and simplification, the fuselage of A320neo was used for the MR-SBW aircraft and taken as the reference for the MR-TF aircraft fuselage sizing. A320neo features a 6-abreast seating arrangement for the economy class. Due to the TF aircraft's fuselage size is scaled down, the seating arrangement for the economy class of the MR-TF aircraft is taken as 4-abreast to ensure the sized cabin meets the cabin design requirements [35]. The two-class cabin layout of the MR-TF aircraft is shown in Fig. 9, with a total of 150 seats, similar to that of A320neo and MR-SBW aircraft. It is worth noting that the nose of the non-cockpit fuselage is arranged with two super-first-class seats with the best view, making full use of the space in the fuselage, providing more choices for passengers, and bring more profits for airlines.

Table 6
Weight breakdown comparison of RHEA-MR aircraft.

Group	MR-SBW	MR-TF	A320neo [39]
Max. takeoff weight, kg	67929	57777	79000
Fuel weight, kg	16127	13328	20980
Empty weight, kg	37582	30229	44300
Empty weight breakdown			
Wing, kg	9393	4631	
Fuselages, kg	7066	5241	
Propulsion, kg	4493	3710	
Nacelles, kg	527	490	
Landing gear, kg	2292	1976	
Horizontal tail, kg	414	772	
Vertical tail, kg	902	844	
Paint, kg	447	415	
Systems, kg	12049	12151	

3.2.2. Aircraft assessment and comparison

As described in Fig. 2, the modified SUAVE, improved for the advanced airframe technologies and SBW and TF aircraft configurations, was used to converge the aircraft weights while satisfying the required flight missions, as shown in Fig. 6 and Table 5. The flight conditions and aircraft configurations of the MR-SBW and MR-TF aircraft obtained during the initial sizing process by PyInit were input into SUAVE for iterative calculations, respectively. The SUAVE analysis results of the RHEA-MR aircraft are listed in Table 6. Besides, the key weight data of the baseline aircraft A320neo [39] is also tabulated in Table 6 for reference and comparison.

As shown in Table 6 and Fig. 10, both SBW and TF configurations with the advanced airframe technologies have significant advantages over the A320neo for the proposed mid-range mission. It is interesting to note that the MR-TF aircraft has significantly better fuel efficiency than that of MR-SBW aircraft, mainly due to the lighter operating empty weight. The load distribution on the MR-TF aircraft wings is more ideal than that of the MR-SBW aircraft because the large centrally positioned fuselage weight is replaced by two outboard positioned weights. Since the pressure cabin skin thickness of a passenger aircraft is proportional to its volume, the total fuselage skin weight of the MR-TF aircraft is lighter than that of the MR-SBW aircraft with the same total fuselage skin area [9], resulting in a lighter total fuselage weight for the MR-TF aircraft. As given in Table 6, on the one hand, the large difference between

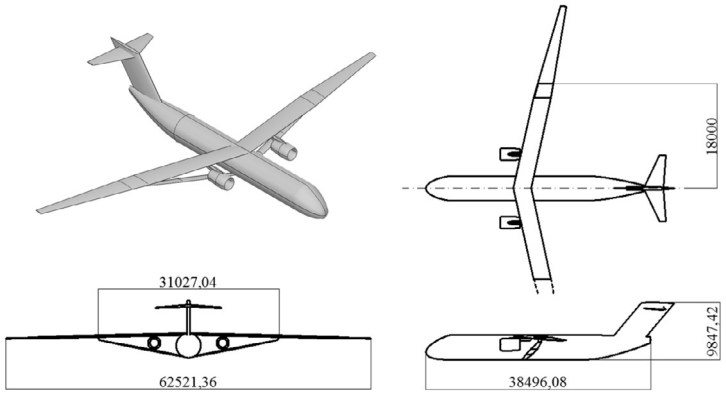

a) MR-SBW

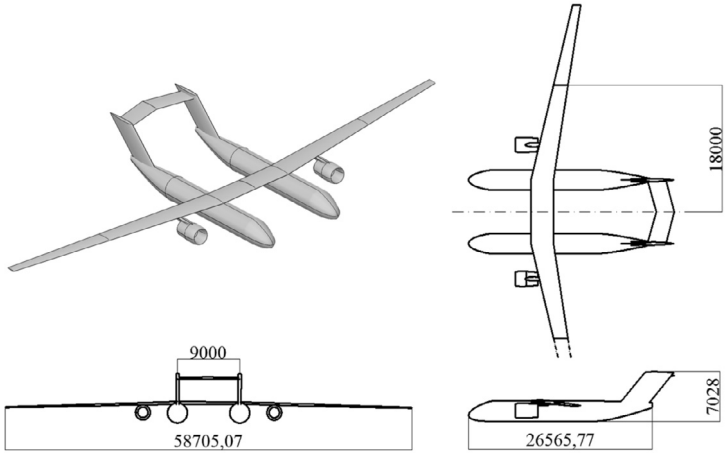

b) MR-TF

Fig. 8. Three-view dimensions of RHEA mid-range aircraft.

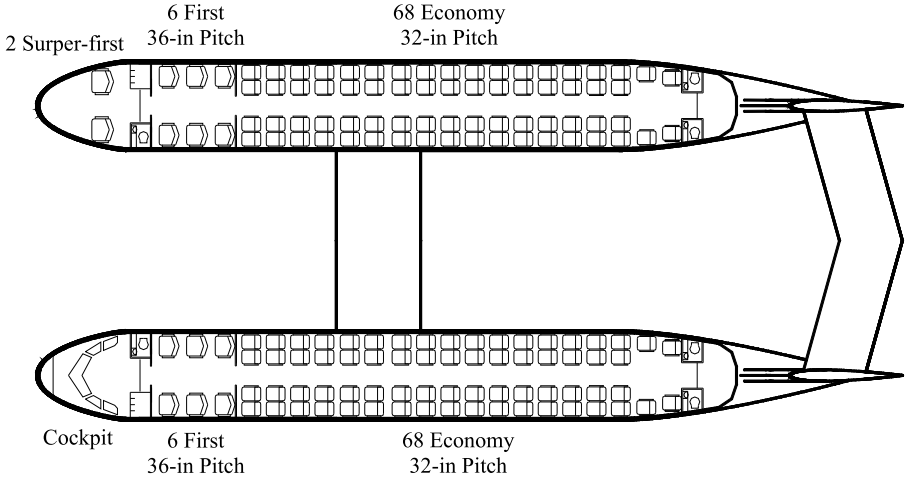

Fig. 9. MR-TF aircraft interior arrangement.

the wing and fuselage weights of the SBW and TF aircraft is due to the explained reasons. On the other hand, it is also due to the smaller TF aircraft MTOW, resulting in a smaller weight per component. Besides, it should be mentioned that the MR-TF aircraft features a heavier horizontal tail because of its shorter fuselage length and shorter tail moment arm, indicating that the forward-swept horizontal tail design is necessary. Otherwise, the horizontal tail would be much heavier.

Then the geometric dimensions of MR-SBW, MR-TF, and several reference aircraft are compared. As shown in Fig. 11, the RHEA-MR aircraft has a larger wingspan than the presented reference aircraft due to the UHARW design. The wingspan of MR-TF aircraft is

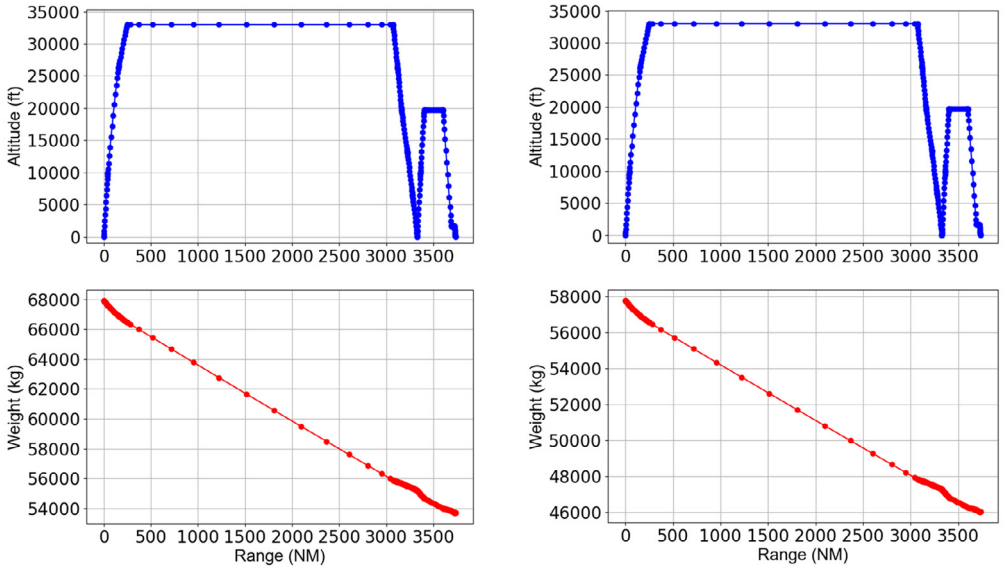

Fig. 10. Mission performance of RHEA-MR aircraft.

Table 7
Top-level requirements of the long-range mission.

Parameter		Unit	RHEA	References			
				VT-SBW [13]	H3.2 [1]	Centerline [40]	DisPURSAL [41]
Reference aircraft		–	B777-300ER	B777-200ER	B777-200LR	A330-300	A330-300
Cruise Mach number		–	0.84	0.85	0.83	0.82	0.8
Max. Mach number		–	0.89				
Passengers (2-class)		–	350			340	340
Passengers (3-class)		–		305	354		
Range		nm	7500	7730	7600	6500	4800
Reserves	Contingency fuel	–	3%		5%		
	Divert segment	nm	200	350			
	Hold (at 1500 ft)	min	10		60		240
Cruise altitude		ft	35000	48000	34921	35000	35000
Service ceiling		ft	40000		40850	41000	
Take-off field length		ft	9000	11000	9000	9514	7546
Landing distance		ft	9000	11000	4966	7874	6562
Approach speed		kt	140	135	156	145	140
Airport (ICAO E)	Wing span	m	65	80 (F)		65	65
	Main landing gear span	m	14				
Certification requirements		–	CS 25	FAR 25	FAR 25	CS 25	

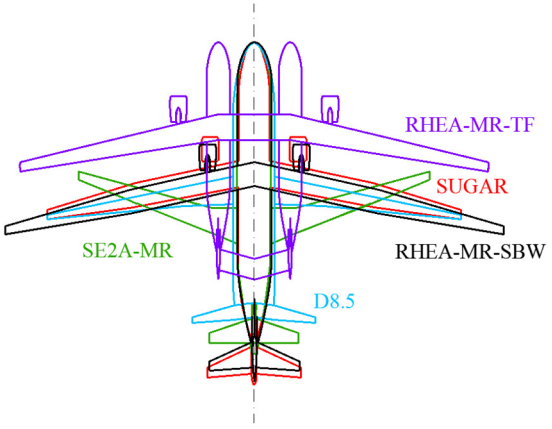

Fig. 11. Geometry comparison of RHEA-MR aircraft.

shorter than that of MR-SBW aircraft because of its lighter MTOW. Due to the TF design, the MR-TF aircraft's fuselage length is significantly less than other aircraft, and its smaller size facilitates airport operations.

Since the MR-TF aircraft's fuselages were sized to have the same total cabin floor area as the reference fuselage, the total volume of the MR-TF aircraft is equal to that of the reference fuselage divided by $\sqrt{2}$, meaning that the MR-TF aircraft's total cargo compartment volume is smaller than that of the reference aircraft, i.e., its cargo capacity is lower. During the TF aircraft sizing process, a constraint was applied to ensure that the luggage weight for each passenger is larger than 23 kg, and the value for the MR-TF aircraft is 23.30 kg.

Therefore, the MR-TF aircraft outperforms the MR-SBW aircraft due to its significant performance advantages and its smaller size. However, it should be noted that this is only the performance results of the initial design configurations based on the reference data and the designer's experience, from which preliminary comparative results can be obtained. Still, it is not enough to comprehensively and accurately reflect the gap between SBW and TF configurations. More precise comparisons and research based on MDO study results are needed in future research.

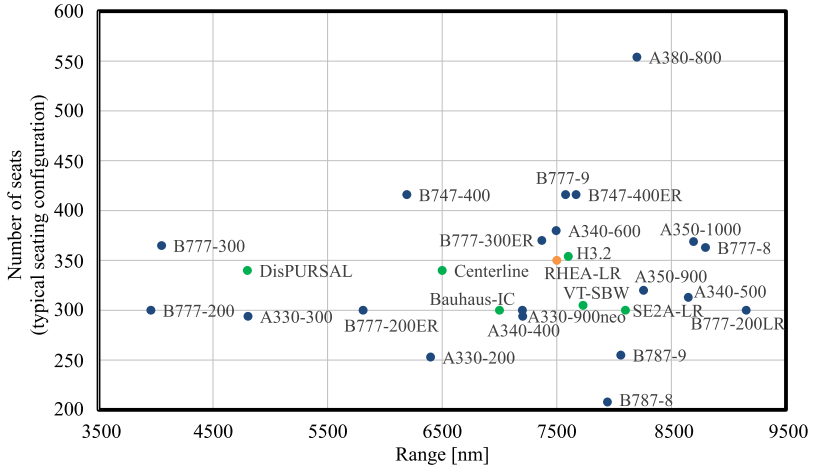

Fig. 12. The number of seats and range of the RHEA-LR aircraft compared to existing aircraft.

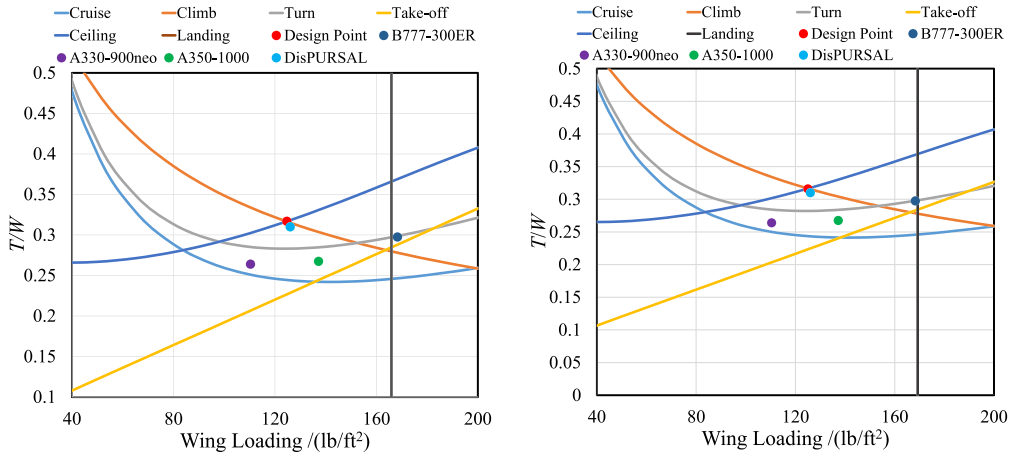

Fig. 13. RHEA-LR aircraft constraint diagrams.

3.3. Long-range mission

3.3.1. Initial aircraft sizing

Similar to the MR mission, several reference passenger aircraft designed for the next-generation LR mission was selected for reference and comparison, including VT-SBW aircraft [13], H3.2 aircraft [1], Centerline aircraft [40], and DisPURSAL aircraft [41]. B777-300ER was selected as the baseline aircraft for the LR mission. The top-level requirements of the RHEA long-range mission and that of the selected reference aircraft are listed in Table 7. A design requirements comparison between the RHEA-LR aircraft (orange dot), the selected reference aircraft (green dots), and numerous existing aircraft (blue dots) are shown in Fig. 12. Besides, the advanced airframe technology assumptions tabulated in Table 4 were applied to PyInit and SUAVE during the LR aircraft conceptual design and performance assessment.

Corresponding to the advanced airframe technology assumptions and the top-level aircraft requirements, the wing loading and thrust-to-weight ratio of the LR-SBW and LR-TF aircraft were sized by PyInit. The design points are shown in Fig. 13. Besides, the design points of the selected reference aircraft are also shown in Fig. 13 for comparison.

Similar to the MR mission considerations, the high-wing configuration with two wing-mounted high bypass ratio turbofan engines was chosen for the LR aircraft, and the wing was designed foldable with the folding position at 65/2 m of the half-wingspan. The same wing and tail airfoils as MR aircraft were initially used for the LR aircraft. A wing sweep angle (0.25c) of 23 deg was chosen as a trade-off between the compressive drag and the laminar flow on the wing surface.

The LR-SBW aircraft features a similar configuration to the MR-SBW aircraft, as shown in Fig. 14. The strut is attached at 58.44% of the half-wingspan position.

The forward-swept high-slab tailplane configuration was initially chosen for the LR-TF aircraft (see “E” in Fig. 15). However, due to the main landing gears’ span limitation (i.e., fuselage spacing) and the short fuselage length, the aspect ratio of the horizontal tail is too small, which will cause poor aerodynamic performance for the horizontal tail. Then, several different horizontal tail configurations were proposed that have more desirable aspect ratios, as shown in Fig. 15. When making trade-offs between these configurations, the main considerations are the aeroelastic and drag (especially compressive drag) of the horizontal tail, and finally, the configuration “F” won out. The three-view dimensions of the final selected LR-TF aircraft configuration are shown in Fig. 16.

The fuselage of the baseline aircraft B777-300ER was used for the LR-SBW aircraft and taken as the reference for the LR-TF aircraft fuselage sizing. The same fuselage sizing method as MR-TF aircraft was used for the LR-TF aircraft fuselage sizing. According to the design requirements in Fig. 12, the LR-SBW and LR-TF aircraft were designed to have the same number of first- and economy-class seats, as shown in Table 8. The reference aircraft B777-300ER

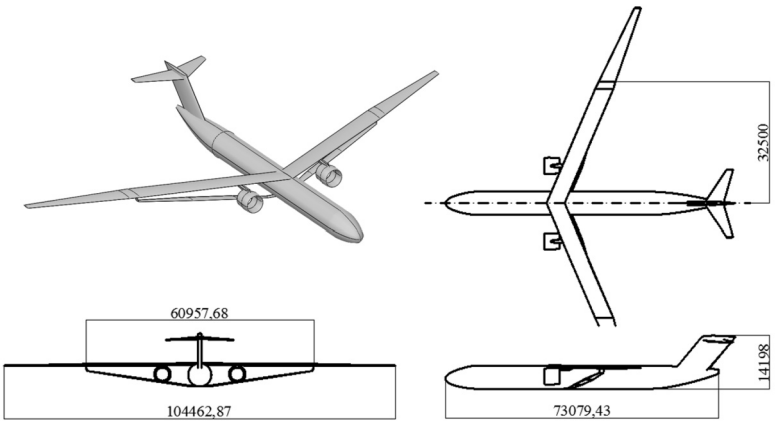

Fig. 14. Three-view dimensions of LR-SBW aircraft.

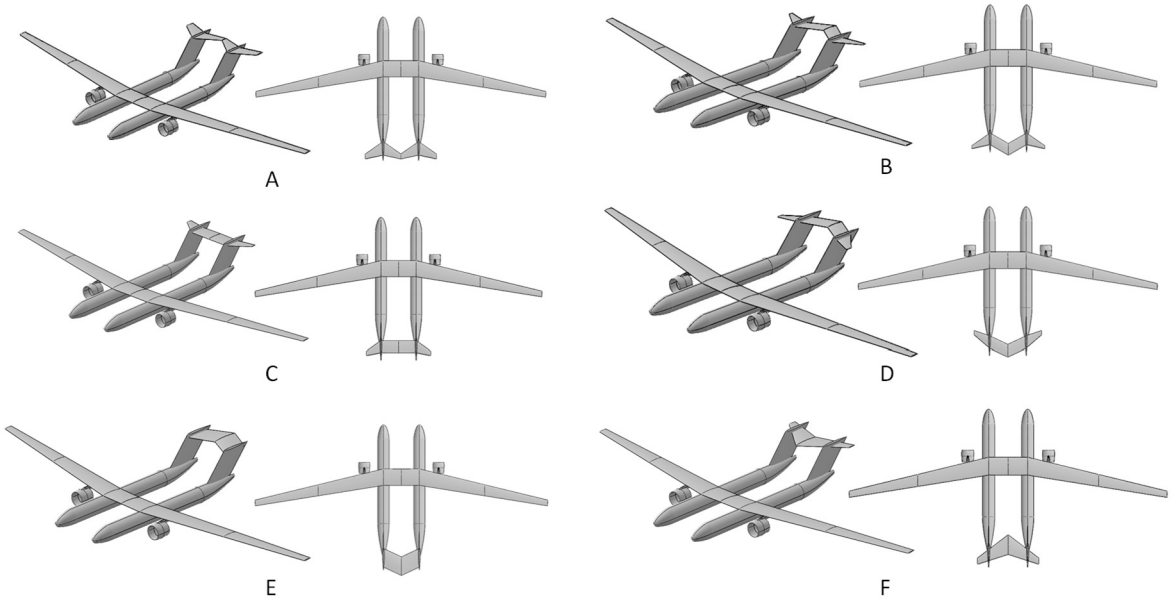

Fig. 15. LR-TF aircraft with different horizontal tail configurations.

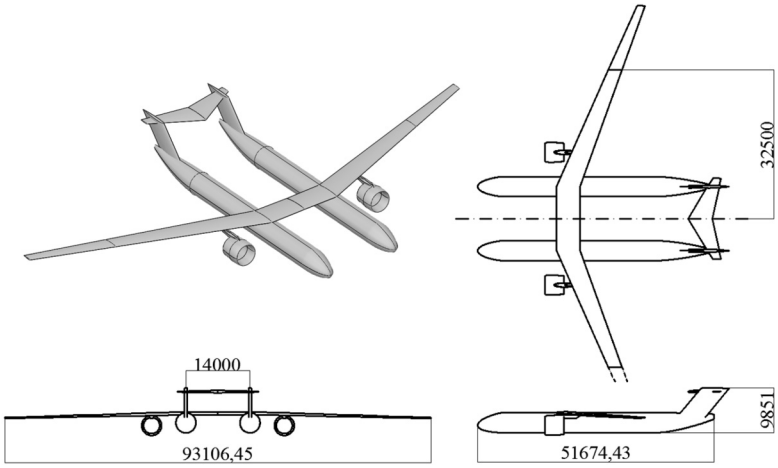

Fig. 16. Three-view dimensions of LR-TF aircraft.

and the LR-SBW aircraft feature a 6-abreast and 9-abreast seating arrangement for the first- and economy-class, respectively, while the LR-TF aircraft has a 4-abreast and 6-abreast seating arrangement for the first- and economy-class, respectively, as shown in Fig. 17. Similar to the MR-TF aircraft's design, the nose of the non-cockpit fuselage is arranged with two super-first-class seats.

The fuselage of the LR-TF aircraft is a circular cross-section, obtained by scaling the fuselage of the B777-300ER, which is a

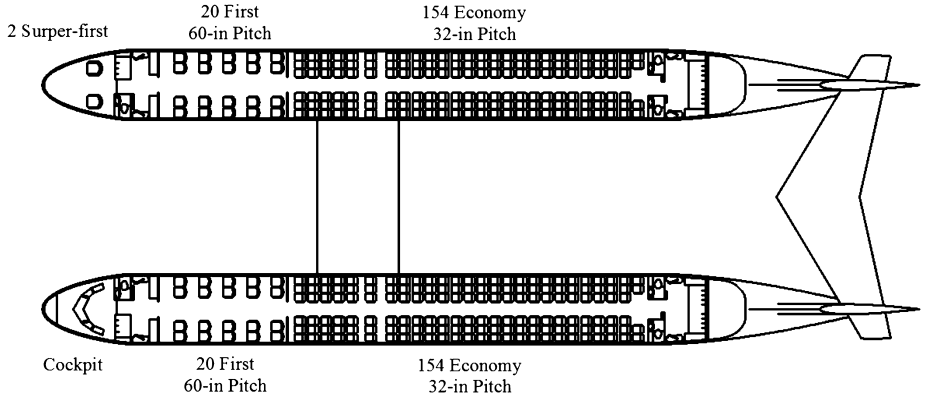

Fig. 17. LR-TF aircraft interior arrangement.

Table 8
Cabin seats number comparison.

Cabin class	LR-SBW	LR-TF
First	42	2+40
Economy	308	308
Total	350	350

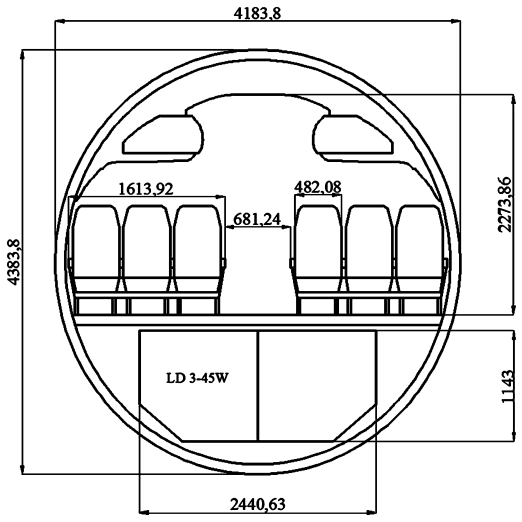

Fig. 18. Fuselage cross-section of LR-TF aircraft.

bit wide for the LR-TF aircraft's 6-abreast economy-class fuselage. Therefore, the width of the LR-TF aircraft fuselage was reduced appropriately to obtain an elliptical cross-section fuselage. The LR-TF aircraft's fuselage cross-section and its cabin parameters are shown in Fig. 18. It is worth noting that the LR-TF aircraft has the same cabin interior arrangement and similar fuselage cross-sectional size as that of A320neo, but the fuselage length is slightly longer. Therefore, the LD3-45W cargo container is selected for the LR-TF aircraft. The cargo capacity per passenger of the LR-TF aircraft is slightly better than that of A320neo and significantly better than that of the MR-TF aircraft.

3.3.2. Aircraft assessment and comparison

The flight conditions and aircraft configurations of the LR-SBW and LR-TF aircraft obtained during the initial sizing by PyInit were input into the modified SUAVE for iterative calculations. The SUAVE analysis results of the LR aircraft and the key weight data of the baseline aircraft B777-300ER [42] are tabulated in Table 9.

As given in Table 9, both SBW and TF configurations with the advanced airframe technologies have significant advantages over

Table 9
Weight breakdown comparison of RHEA-LR aircraft.

Group	LR-SBW	LR-TF	B777-300ER [42]
Max. takeoff weight, kg	262962	210955	351535
Fuel weight, kg	89716	80037	145538
Empty weight, kg	140066	97737	167829
Empty weight breakdown			
Wing, kg	47401	16630	
Fuselages, kg	25757	20596	
Propulsion, kg	18650	15038	
Nacelles, kg	2460	2270	
Landing gear, kg	7023	5735	
Horizontal tail, kg	1483	1478	
Vertical tail, kg	2923	2392	
Paint, kg	1237	1153	
Systems, kg	33133	32446	

the B777-300ER for the proposed long-range mission shown in Fig. 19. The results are similar to the MR mission in that the TF aircraft has a better fuel efficiency due to its lighter operating empty weight than the SBW configuration. It is worth noting that the difference in wing weight between the LR-SBW and LR-TF aircraft is greater than that of the MR aircraft, which is due to the better unloading effect on the wing due to the heavier outboard positioned fuselages. Besides, due to the smaller fuselage equivalent diameter, the LR-TF aircraft fuselage is also lighter than that of the LR-SBW aircraft.

As shown in Fig. 20, the geometric dimensions of LR-SBW, LR-TF, and B777-300ER are compared. Due to the UHARW design, the RHEA-LR aircraft's wings need to be designed as foldable, as marked in the figure. It should be noted that both the wingspan and the fuselage length of the LR-TF aircraft are smaller than those of the LR-SBW aircraft because of its smaller MTOW and the TF concept characteristics.

Therefore, the LR-TF aircraft outperforms the LR-SBW aircraft due to its obvious performance advantages and smaller size. It should be noted that this comparison result was only based on the initial conceptual design results, which may not be enough to reflect the differences between these two unconventional configurations, and the further MDO study needs to be carried out in the following research stage.

3.4. Short-range mission

3.4.1. Initial aircraft sizing

Several reference passenger aircraft designed for the next-generation Short-Range mission, including Saeed-007.1 [6], PEGASUS [43], TU Delft [44], and TPR70neo+ [45], were chosen for reference and comparison. ATR72-600 was selected as the baseline aircraft for the SR mission. The top-lever requirements of the RHEA

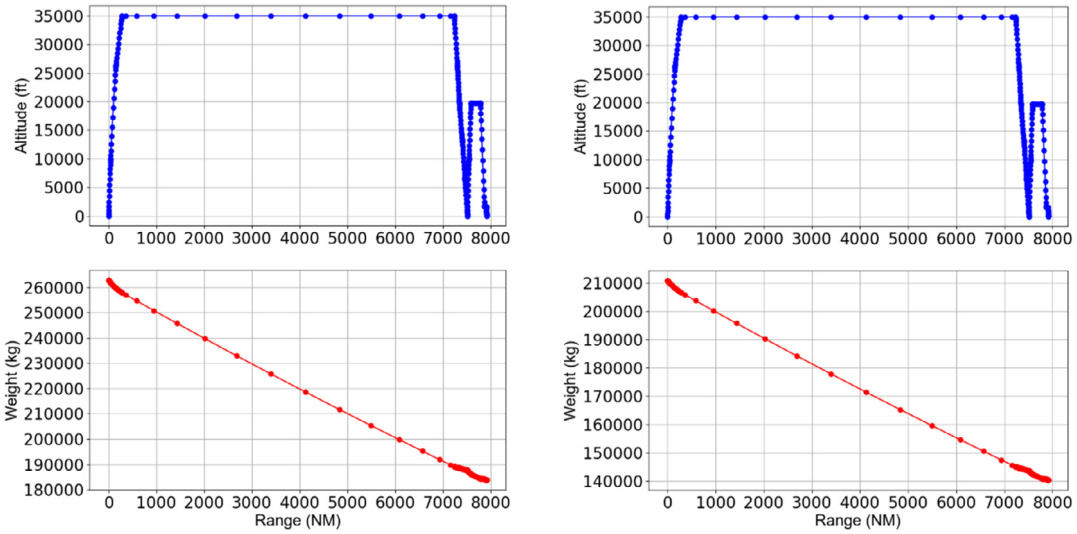

Fig. 19. Mission performance of RHEA-LR aircraft.

Table 10
Top-level requirements of the short-range mission.

Parameter		Unit	RHEA	References			
				Saeed-007.1 [6]	PEGASUS [43]	TU-Delft [44]	TPR70neo+ [45]
Reference aircraft		–	ATR 72-600	ATR 42/72	ATR72-500	ATR 72-600	ATR 72 & Dash 8
Propulsion concept		–	Turboprop	Turbofan	Hybrid	Hybrid	Turboprop
Cruise Mach number		–	0.42	0.457	0.45	0.415	0.41
Max. Mach number		–	0.457	0.5		0.457	0.55
Passengers		–	72	72	48	70	70
Range		nm	825	1242	400	825	826
Reserves	Contingency fuel	–	3%	0			
	Divert segment	nm	87	270	87		
	Hold (at 1500 ft)	min	10	0	45		
Cruise altitude		ft	20000	20000	20000	25000	23000
Service ceiling		ft	25000		25000	25000	
Take-off field length		ft	4373	4265			4429
Landing distance		ft	3002				2917
Approach speed		kt	113	120			118
Airport category (ICAO C)	Wingspan	m	36				36
	Main landing gear span	m	9				9
Certification requirements		–	CS 25		Part 25	CS 25	CS 25

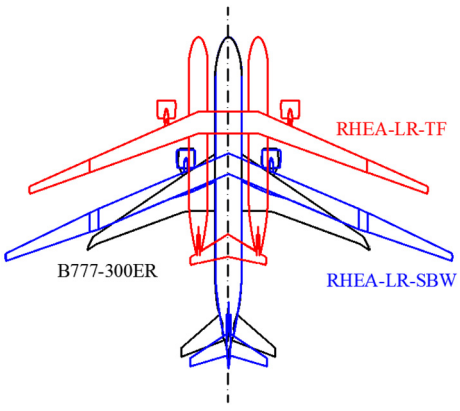

Fig. 20. Geometry comparison of RHEA-LR aircraft.

short-range mission and those of the selected reference aircraft are tabulated in Table 10. Besides, the advanced airframe technologies assumed in Table 4 were applied to PyInit and SUAVE for the SR aircraft conceptual design and performance analysis.

It should be noted that turboprop engines were used for the RHEA-SR aircraft, so the PyInit was extended to take into account the power-to-weight ratio (P/W) for this kind of aircraft. Corresponding to the advanced airframe technology assumptions and the top-level aircraft requirements, the wing loading and power-to-weight ratio of the SR-SBW and SR-TF aircraft were sized by the improved PyInit, and the design points are shown in Fig. 21. Besides, the design points of the chosen reference aircraft are also shown in Fig. 21 for comparison.

Because of the UHARW design, the high-wing configuration with two turboprop engines was chosen for the SR aircraft, and the wing is designed foldable with the folding position at 36/2 m of the half-wingspan. Since the SR aircraft will operate in the subsonic region, NACA 65-618 and NACA 65-613 were selected for the wing roots and tips to maximize laminar flow, and NACA 0010 airfoil was chosen for tailplanes. A straight wing was designed to maximize the wing's aerodynamic performance according to the subsonic operating condition.

Most short-range aircraft use the wing-mounted engine configuration or aft-mounted engine configuration, as shown in Fig. 22. From the aerodynamic point of view, the aft-mounted turboprop

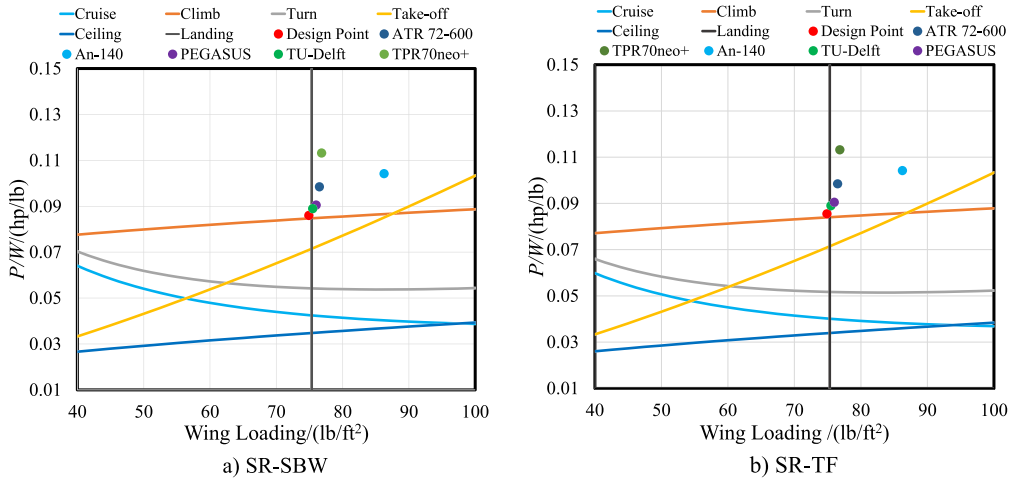

Fig. 21. RHEA-SR aircraft constraint diagrams.

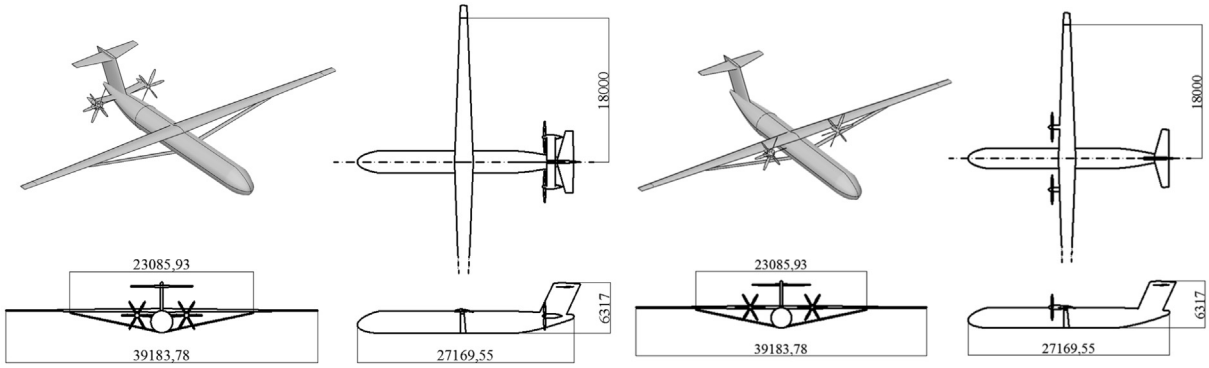

Fig. 22. Three-view dimensions of SR-SBW aircraft with aft-mounted engines (left) and wing-mounted engines (right).

engine configuration is preferable because a completely clean wing enables a substantially laminar flow percentage. In contrast, it is challenging to maintain laminar flow in the wing region affected by the propeller downwash of the configuration with wing-mounted engines. However, since SBW aircraft usually have a high-wing configuration, the aft-mounted propellers' incoming flow is not uniform (i.e., contains both free stream and wing wake flow). The propeller's fatigue life and its overall vibrations introduced into the pylon and nacelle will be obvious issues. Besides, this concept may also have problems with control at low speeds, which is possible due to the unsteady flow into the propeller. While for the wing-mounted engine configuration, engines and propellers will operate in an ideal working condition and the wing-mounted engines are conducive to unloading the wing. Therefore, after comparative analysis, the wing-mounted engine configuration was selected for the SR-SBW aircraft (the right one in Fig. 22), which is not as good as the aft-mounted engine configuration in terms of laminar flow maintenance but has no serious problems. Besides, the strut is attached at 60% of the half-wingspan position.

The wing-mounted engines and forward-swept high-slab tailplane configuration were initially selected for the SR-TF aircraft (see "A" in Fig. 23). Due to the wide fuselage spacing, the horizontal tail aspect ratio is too large. Thus some structural aspect problems may arise, and the wing laminar flow proportion is not maximized. When separating the horizontal tail to each fuselage and moving the engines to the fuselage tail, the configuration "E" is obtained. However, the asymmetric engine concept will produce unexpected torque to the fuselage structure. When the engine pylons are attached by a low-slab tailplane (see "B" in Fig. 23), the unexpected torque can be significantly reduced. Still, the horizontal tail area will increase, resulting in increased takeoff weight. A good solution is to mount the engines at the joint of the vertical and horizontal tails of the twin tee-tail configuration "D" or canted slab-tail configuration "F". However, such engine positions will introduce additional pitch-down moments to the aircraft. Therefore, the wing-mounted engines and twin tee-tail configuration were selected for the initial conceptual design and configuration comparative study. Other configurations will be further investigated and compared in future studies, if necessary. The three-view dimensions of the final selected SR-TF aircraft configuration are shown in Fig. 24.

The fuselage of the reference aircraft ATR 72-600 was used for the SR-SBW aircraft and taken as the reference for the SR-TF aircraft fuselage sizing. The same fuselage sizing methodology as MR-TF aircraft was used. According to the top-level requirements, the SR-SBW and SR-TF aircraft were designed to have the same number of total seats as the ATR 72-600, i.e., 72 seats [46]. The reference aircraft ATR 72-600 and the SR-SBW aircraft feature a 4-abreast and 29-in pitch seating arrangement (see Fig. 25). After scaling down from the reference fuselage, the width of the TF aircraft fuselage could accommodate 3-abreast seats, but the cabin aisle height cannot meet the requirements. Therefore, the fuselage width was manually reduced to include a 2-abreast seating arrangement. The fuselage cross-section's height was slightly increased to the same height as the reference fuselage. The sized fuselage cross-section and its cabin parameters are shown in Fig. 26 and Table 11, which feature an elliptical cross-section.

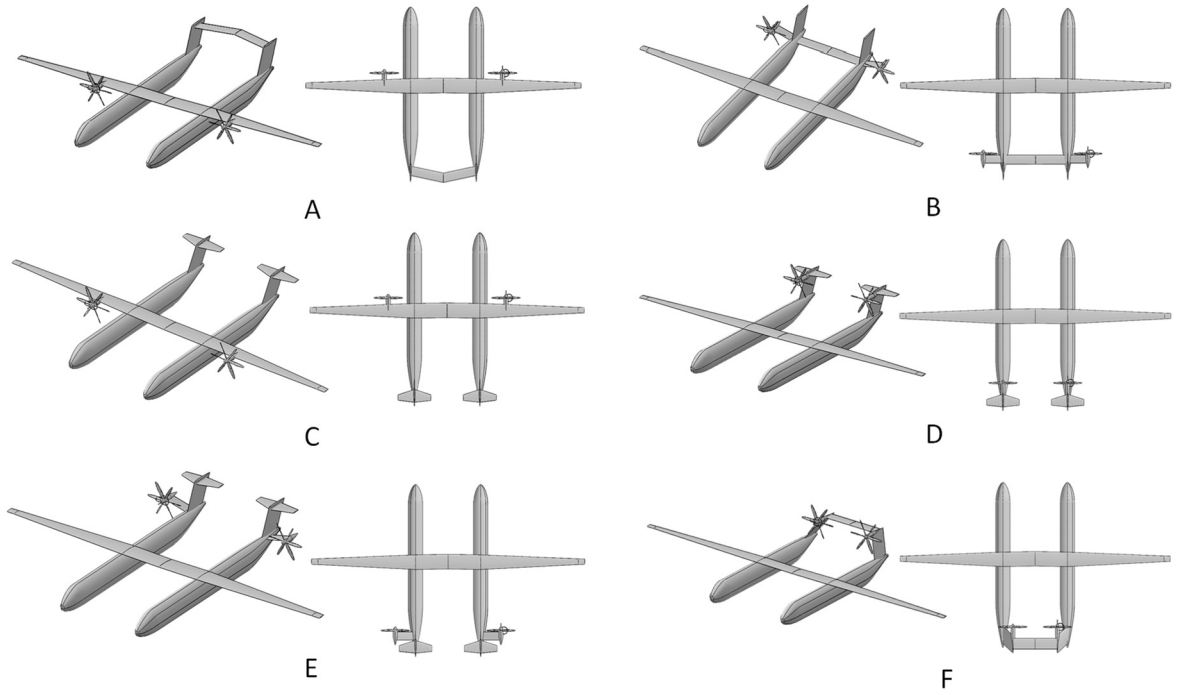

Fig. 23. Different SR-TF aircraft configurations.

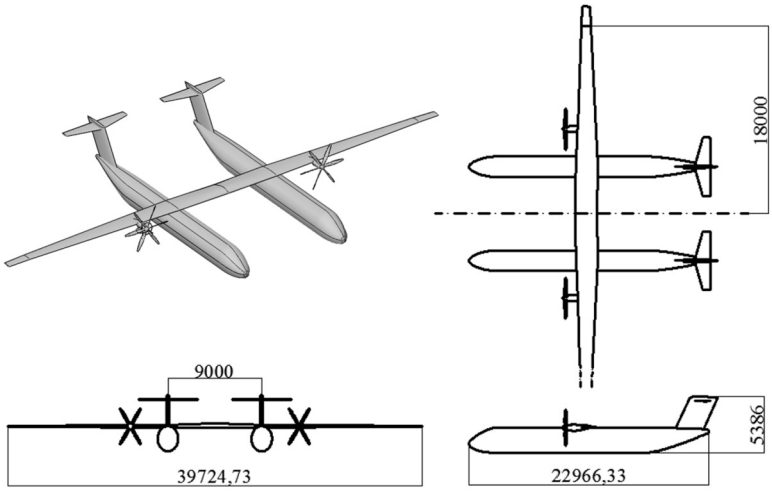

Fig. 24. Three-view dimensions of SR-TF aircraft.

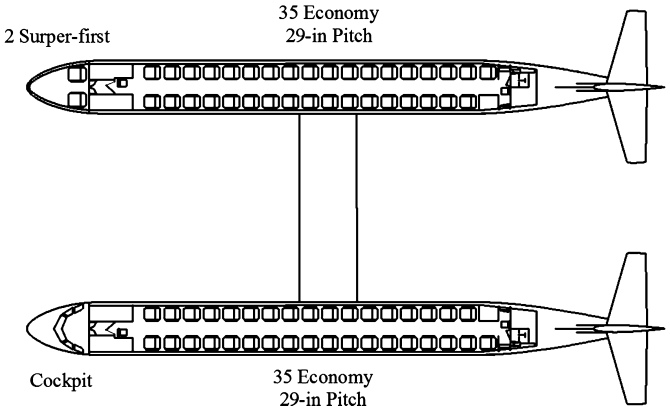

Fig. 25. SR-TF aircraft interior arrangement.

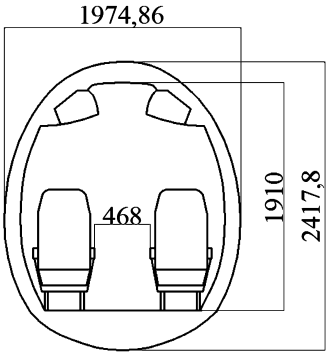

Fig. 26. Fuselage cross-section of SR-TF aircraft.

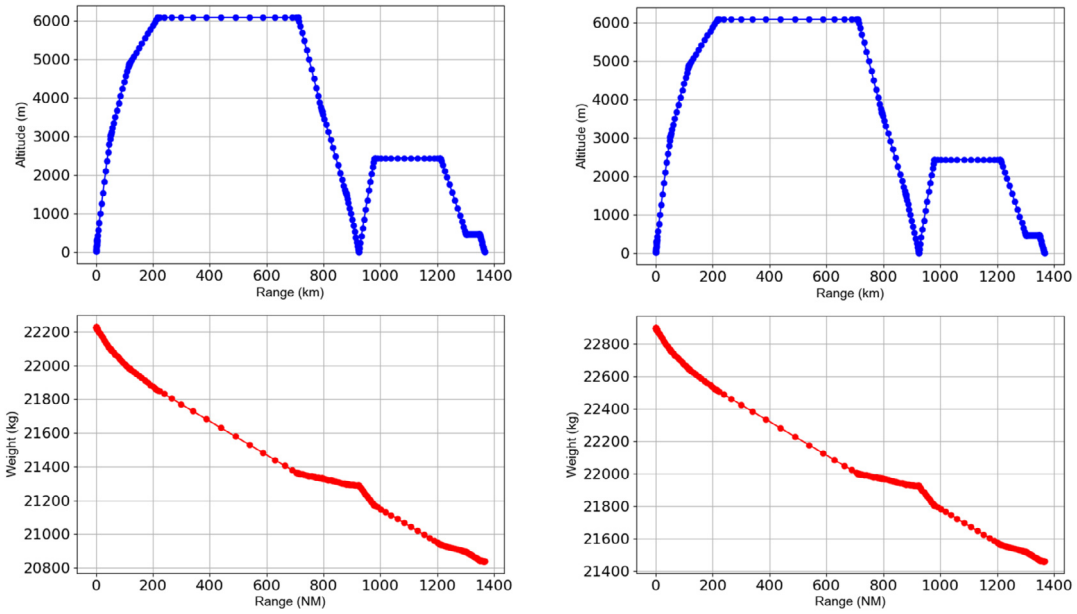

a) SR-SBW b) SR-TF

Fig. 27. Mission performance of RHEA-SR aircraft.

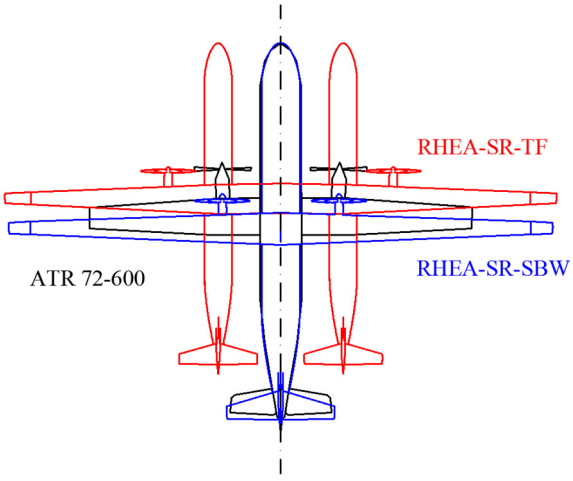

Fig. 28. Geometry comparison of RHEA-SR aircraft.

Table 11
Cabin parameters of SR-TF aircraft.

Parameter	SR-TF	ATR 72-600 [46]
Pitch, in	29	29
Seat width, in	18.6	18.6
Aisle width, in	18.4	18.4
Aisle height, in	75.2	75.2
Cabin floor width, in	51.6	89
Floor thickness, in	4	4

3.4.2. Aircraft assessment and comparison

The flight conditions and aircraft configurations of the SR-SBW and SR-TF aircraft obtained during the initial sizing by PyInit were input into the modified SUAVE for performance analysis through iterative calculations. The SUAVE analysis results of the SR aircraft and the key weight data of the reference aircraft ATR 72-600 [46] are given in Table 12.

Table 12
Weight breakdown comparison of RHEA-SR aircraft.

Group	SR-SBW	SR-TF	ATR 72-600 [46]
Max. takeoff weight, kg	22229	22945	22800
Fuel weight, kg	1432	1523	2000
Empty weight, kg	12821	13447	13500
Empty weight breakdown			
Wing, kg	2103	1482	
Fuselages, kg	2497	3052	
Propulsion, kg	1019	1047	
Nacelles, kg	269	275	
Landing gear, kg	643	661	
Horizontal tail, kg	201	214	
Vertical tail, kg	312	326	
Paint, kg	199	240	
Systems, kg	5579	6150	

As listed in Table 12, both the SR-SBW and SR-TF configurations with the advanced airframe technologies have a significant advantage in fuel efficiency over the reference ATR 72-600 for the proposed short-range mission shown in Fig. 27 (both reduce fuel consumption by more than 20%). However, it is interesting to note that the MTOW, fuel weight, and operating empty weight of the SR-TF aircraft are larger than those of the SR-SBW aircraft, contrary to the MR and LR missions' results. The empty weight breakdown in Table 12 shows that the wing weight of the SR-TF aircraft configuration is still lighter than that of the SR-SBW aircraft, but the weight of the fuselage and the fuselage-related items, including paint and systems, is greater than that of the SR-SBW aircraft, due to the larger fuselage size of the manually modified SR-TF aircraft, which offsets the wing weight savings.

As shown in Fig. 28, the geometric dimensions of SR-SBW, SR-TF, and ATR 72-600 are compared. Due to the UHARW design, the RHEA-SR aircraft's wings need to be designed as foldable, as marked in the figure. The SR-TF aircraft fuselage is shorter than that of the SR-SBW aircraft, but it has a slightly larger wingspan due to its higher takeoff weight.

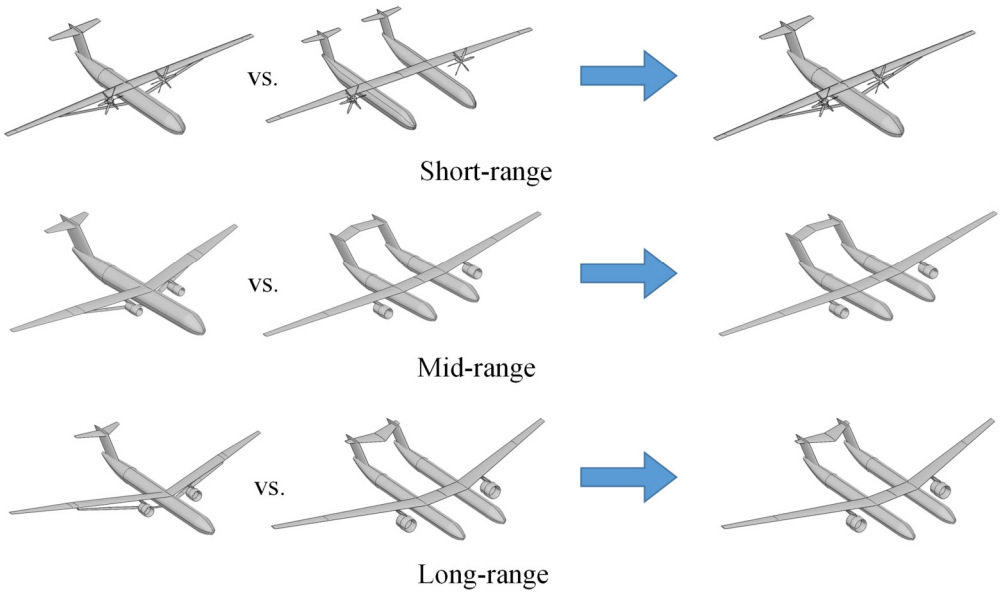

Fig. 29. RHEA aircraft configuration selection process.

Therefore, for the SR mission, the SBW configuration performs better than the TF configuration due to the better fuel efficiency, lighter takeoff weight, smaller wingspan, etc. In future studies, the other TF configurations in Fig. 23 will be compared with the SBW configuration to investigate whether the SBW configuration still has better performance for the SR mission.

In summary, the SBW configuration and TF configuration initially proposed for each mission in this section and the final selected one are shown in Fig. 29.

4. Conclusion

This paper addressed the conceptual design and comparative study of two unconventional aircraft configurations that facilitate the UHARW design, including the SBW configuration and the TF configuration. Several tools were used in this work for the aircraft conceptual design and performance analysis, which were modified and improved for the SBW and TF configurations and the advanced airframe technologies assumed to be available at the EIS framework of the researched aircraft. According to the proposed mission profile and top-level requirements, an SBW and a TF configuration were designed for each mission, respectively, and a comparative study was carried out to determine the best-case configuration for the corresponding mission.

For all three missions researched in this paper (i.e., SR, MR, and LR missions), the TF configuration has a more significant weight reduction effect on the wing weight than that of the SBW configuration, making the MR-TF and LR-TF aircraft perform better than the SBW configuration. However, for the SR mission, considering the specific arrangement of the passenger cabin, the fuselage size had to be adjusted, increased the total fuselage wetted area and resulting in a higher weight increase of the fuselage and associated systems, thus resulting in the SR-TF aircraft performance inferior to that of the SR-SBW aircraft.

The smaller individual fuselage size of the TF aircraft results in a weaker cargo capacity than that of the SBW configuration. The MR-TF aircraft can barely meet the minimum passenger luggage requirements. While the LR-TF aircraft's situation is slightly better, it is still far inferior to the conventional and SBW configurations.

There are constraints on the aircraft wingspan and main landing gear span when the aircraft operates at ICAO airports. Due to the TF aircraft characteristics, its fuselage spacing is constrained by the main landing gear span, which brings both new possibilities and restrictions to the TF aircraft's horizontal tail configuration design. The TF aircraft horizontal tail design requires trade-offs in terms of aerodynamic efficiency, aeroelastic performance, weight, etc. In this paper, three completely different horizontal tail configurations were used for the three TF aircraft due to their different operating conditions and fuselage spacing.

This work preliminarily researched the potential of the SBW configuration and the TF configuration for the next-generation passenger aircraft with UHARW design. The wing weight estimation methods used in this paper for SBW and TF configurations were Class II and Class II & 1/2, respectively, which have been validated in this paper, and the accuracy is acceptable and feasible for the conceptual design stage. In future work, more accurate wing weight estimation methods will be developed for SBW and TF configurations, and aeroelasticity and flutter analysis will be introduced for UHARW for a detailed comparative study of these two unconventional configurations. Besides, the configuration comparative research results obtained in this paper were based on the initial conceptual design results. Multidisciplinary design optimization research will be conducted for each concept in the next stage, and then the optimum SBW configuration and TF configuration will be compared again for each mission to observe whether the best-case and worst-case configuration will change.

Declaration of competing interest

The authors declare that they have no known competing financial interests or personal relationships that could have appeared to influence the work reported in this paper.

Acknowledgements

This project has received funding from the Clean Sky 2 Joint Undertaking (JU) under grant agreement No 883670. The JU receives support from the European Union's Horizon 2020 research and innovation programme and the Clean Sky 2 JU members other than the Union. The authors would like to thank Rafael Palacios (Imperial College London) and Rolf Radespiel (Technische Universität Braunschweig) for their feedback on the aircraft configuration design.

References

[1] E.M. Greitzer, P.A. Bonnefoy, E. De la Rosa Blanco, C.S. Dorbian, M. Drela, D.K. Hall, et al., N+3 aircraft concept designs and trade studies, final report, NASA/CR-2010-216794/vol2, NASA Glenn Research Center, Cleveland, Ohio, 2010, 44135.

[2] Advisory Council for Aviation Research and Innovation in Europe-ACARE, Realising Europe's vision for aviation, Strategic Research & Innovation Agenda, vol. 1, 2012.

[3] M. Wu, Z. Shi, T. Xiao, et al., Effect of wingtip connection on the energy and flight endurance performance of solar aircraft, Aerosp. Sci. Technol. 108 (2021) 106404, https://doi.org/10.1016/j.ast.2020.106404.

[4] J.G. Coder, D.M. Somers, Design of a slotted, natural-laminar-flow airfoil for commercial transport applications, Aerosp. Sci. Technol. 106 (2020) 106217, https://doi.org/10.1016/j.ast.2020.106217.

[5] Y.V. Vedernikov, V.E. Chepiga, V.P. Maslakov, E.A. Kuklev, V.G. Gusev, Configuration of the medium-haul twin-fuselage passenger aircraft, Int. J. Appl. Eng. Res. 12 (4) (2017) 414–421.

[6] S. Hosseini, M. Ali Vaziri-Zanjani, H. Reza Ovesy, Conceptual design and analysis of an affordable truss-braced wing regional jet aircraft, Proc. Inst. Mech. Eng., G J. Aerosp. Eng. 0954410020923060 (2020), https://doi.org/10.1177/0954410020923060.

[7] F. Torrigiani, J. Bussemaker, P.D. Ciampa, M. Fioriti, F. Tomasella, B. Aigner, et al., Design of the strut braced wing aircraft in the agile collaborative MDO framework, in: 31st Congress of the International Council of the Aeronautical Sciences, Belo Horizonte, Brazil, 2018.

[8] M.K. Bradley, C.K. Droney, T.J. Allen, Subsonic Ultra Green Aircraft Research: Phase II – Volume I – Truss Braced Wing Design Exploration, NASA/CR–2015-218704/Volume I, 2015.

[9] E. Torenbeek, Advanced Aircraft Design: Conceptual Design, Analysis and Optimization of Subsonic Civil Airplanes, John Wiley and Sons Ltd, West Sussex, 2013.

[10] Y. Ma, W. Zhang, Y. Zhang, X. Zhang, Y. Zhong, Sizing method and sensitivity analysis for distributed electric propulsion aircraft, J. Aircr. 57 (4) (2020) 730–741, https://doi.org/10.2514/1.C035581.

[11] J. Kallo, DLR leads HY4 project for four-seater fuel cell aircraft, Fuel Cells Bull. 2015 (11) (2015) 13, https://doi.org/10.1016/S1464-2859(15)30362-X.

[12] M. Guerster, E.F. Crawley, Dominant suborbital space tourism architectures, J. Spacecr. Rockets 56 (5) (2019) 1580–1592, https://doi.org/10.2514/1.A34385.

[13] K.H. Khan, W. Mallik, R.K. Kapania, J.A. Schetz, Distributed Design Optimization of Large Aspect Ratio Wing Aircraft with Rapid Transonic Flutter Analysis in Linux, AIAA Paper 2021-1354, Jan. 2021.

[14] S. Karpuk, A. Elham, Conceptual Design Trade Study for an Energy-Efficient Mid-Range Aircraft with Novel Technologies, AIAA Paper 2021-0013, Jan. 2021.

[15] N. Beck, T. Landa, A. Seitz, L. Boermans, Y. Liu, R. Radespiel, Drag reduction by laminar flow control, Energies 11 (1) (2018) 252, https://doi.org/10.3390/en11010252.

[16] B. Mele, L. Russo, R. Tognaccini, Drag bookkeeping on an aircraft with riblets and NLF control, Aerosp. Sci. Technol. 98 (2020) 105714, https://doi.org/10.1016/j.ast.2020.105714.

[17] C.C. Rossow, H. Von Geyr, M. Hepperle, The 1g-Wing, Visionary Concept or Naive Solution?, DLR-IB-AS-BS-2016-121, 2016.

[18] T.R. Brooks, J.R. Martins, G.J. Kennedy, High-fidelity aerostructural optimization of tow-steered composite wings, J. Fluids Struct. 88 (2019) 122–147, https://doi.org/10.1016/j.jfluidstructs.2019.04.005.

[19] P. Horst, A. Elham, R. Radespiel, Reduction of aircraft drag, loads and mass for energy transition in aeronautics, in: DLRK 2020, Sept. 2020.

[20] A. Elham, R. Radespiel, M. Fossati, R. Palacios, A. Gazaix, K. Artois, RHEA: robust by design ultra high aspect ratio wing and airframe, in: 10th EASN Conference, 2020.

[21] T.W. Lukaczyk, A.D. Wendorff, M. Colonno, T.D. Economon, J.J. Alonso, T.H. Orra, C. Ilario, SUAVE: an Open-Source Environment for Multi-Fidelity Conceptual Vehicle Design, AIAA Paper 2015-3087, June 2015.

[22] G.P. Chiozzotto, Initial weight estimate of advanced transport aircraft concepts considering aeroelastic effects, AIAA Paper 2017-0009, Jan. 2017.

[23] S.V. Udin, W.J. Anderson, Wing mass formula for twin fuselage aircraft, J. Aircr. 29 (5) (1992) 907–914, https://doi.org/10.2514/3.46261.

[24] O. Gur, M. Bhatia, W.H. Mason, J.A. Schetz, R.K. Kapania, T. Nam, Development of a framework for truss-braced wing conceptual MDO, Struct. Multidiscip. Optim. 44 (2) (2011) 277–298, https://doi.org/10.1007/s00158-010-0612-9.

[25] A. De Marco, M. Di Stasio, P. Della Vecchia, V. Trifari, F. Nicolosi, Automatic modeling of aircraft external geometries for preliminary design workflows, Aerosp. Sci. Technol. 98 (2020) 105667, https://doi.org/10.1016/j.ast.2019.105667.

[26] D.P. Wells, B.L. Horvath, L.A. McCullers, The flight optimization system weights estimation method, NASA/TM–2017–219627/Volume I, NASA Langley Research Center, Hampton, Virginia, 2017.

[27] G. Carrier, O. Atinault, S. Dequand, et al., Investigation of a strut-braced wing configuration for future commercial transport, in: 28th Congress of the International Council of the Aeronautical Sciences, ICAS, Bonn, 2012.

[28] N.A. Harrison, G.M. Gatlin, S.A. Viken, M. Beyar, E.D. Dickey, K. Hoffman, E.Y. Reichenbach, Development of an Efficient M = 0.80 Transonic Truss-Braced Wing Aircraft, AIAA Paper 2020-0011, Jan. 2020.

[29] L.P. Metkowski, M. Maughmer, Winglet and Strut Configuration Study for a Slotted, Natural-Laminar-Flow Strut-Braced Transport Aircraft, AIAA paper 2021-0843, Jan. 2021.

[30] X.T. Zhang, S. Zhang, J.L. Wang, et al., Effect of primary parameters on structure weight of civil aircraft with strut-braced wing, Acta Aeronaut. Astronaut. Sin. 40 (2) (2019) 522359, https://doi.org/10.7527/S1000-6893.2018.22359 (in Chinese).

[31] A. Elham, M.J.L. van Tooren, Effect of wing-box structure on the optimum wing outer shape, Aeronaut. J. 118 (1199) (2014) 1–30, https://doi.org/10.1017/S0001924000008903.

[32] L.J. Hart-Smith, The ten-percent rule for preliminary sizing of fibrous composite structures, Weight Eng. 52 (2) (1992) 29–45.

[33] Y. Ma, A. Elham, Twin-fuselage configuration for improving fuel efficiency of passenger aircraft, Aerosp. Sci. Technol. 118 (2021) 107000, https://doi.org/10.1016/j.ast.2021.107000.

[34] Certification Specifications and Acceptable Means of Compliance for Large Aeroplanes CS-25, https://www.easa.europa.eu/document-library/certification-specifications/cs-25-amendment-25, June 2020.

[35] D. Raymer, Aircraft design: a conceptual approach, 6th edition, in: AIAA Education Series, American Institute of Aeronautics and Astronautics, Washington, DC, 2018.

[36] J. Moore, D. Maddalon, Multibody Transport Concept, AIAA Paper 1982-0810, May 1982.

[37] B.M. Yutko, N. Titchener, C. Courtin, M. Lieu, L. Wirsing, J. Tylko, et al., Conceptual design of a D8 commercial aircraft, AIAA Paper 2017-3590, June 2017.

[38] M.K. Bradley, C.K. Droney, Subsonic ultra green aircraft research: phase I final report, NASA/CR–2011-216847, Langley Research Center, NASA, 2011.

[39] S.A.S. Airbus, A320 Aircraft Characteristics Airport and Maintenance Planning, Issue: 30 Sept. 1985, Rev: 1 April 2020.

[40] F. Troeltsch, J. Bijewitz, A. Seitz, Design trade studies for turbo-electric propulsive fuselage integration, in: Proceedings of the 24th ISABE Conference, International Society for Air Breathing Engines, Canberra, Australia, Sept. 2019, pp. 22–27.

[41] A.T. Isikveren, A. Seitz, J. Bijewitz, A. Mirzoyan, A. Isyanov, R. Grenon, et al., Distributed propulsion and ultra-high by-pass rotor study at aircraft level, Aeronaut. J. 119 (1221) (2015) 1327–1376.

[42] B.C. Airplanes, 777-200LR/-300ER/-freighter airplane characteristics for airport planning, Document Number D6-58329-2, http://www.boeing.com/assets/pdf/commercial/airports/acaps/777_2lr3er.pdf, 2015.

[43] N.J. Blaesser, Z.J. Frederick, Tail Sizing Considerations for Wingtip Propulsor Driven Aircraft Applied to the Parallel Electric-Gas Architecture with Synergistic Utilization Scheme (PEGASUS) Concept, AIAA Paper 2020-2633, June 2020.

[44] M. Voskuijl, J. Van Bogaert, A.G. Rao, Analysis and design of hybrid electric regional turboprop aircraft, CEAS Aeronaut. J. 9 (1) (2017) 15–25, https://doi.org/10.1007/s13272-017-0272-1.

[45] M. Strack, G. Pinho Chiozzotto, M. Iwanizki, M. Plohr, M. Kuhn, Conceptual Design Assessment of Advanced Hybrid Electric Turboprop Aircraft Configurations, AIAA Paper 2017-3068, June 2017.

[46] ATR-72 Series 600 Brochure. Available online https://perma.cc/95KA-S7XS, 2014. (Accessed 2 January 2021).